

UNCLASSIFIED

AD 408 797

DEFENSE DOCUMENTATION CENTER

FOR

SCIENTIFIC AND TECHNICAL INFORMATION

CAMERON STATION, ALEXANDRIA, VIRGINIA



UNCLASSIFIED

NOTICE: When government or other drawings, specifications or other data are used for any purpose other than in connection with a definitely related government procurement operation, the U. S. Government thereby incurs no responsibility, nor any obligation whatsoever; and the fact that the Government may have formulated, furnished, or in any way supplied the said drawings, specifications, or other data is not to be regarded by implication or otherwise as in any manner licensing the holder or any other person or corporation, or conveying any rights or permission to manufacture, use or sell any patented invention that may in any way be related thereto.

RADC-TN-61-242

Development of

**A Very Low Noise  
Traveling-Wave Tube.**

Scientific Report No. 1,

Covering the Period

January 8 to March 15, 1960

Prepared by

G. Hodowanec

H. Wolkstein

Approved by

M. Nowogrodzki

For

Radio Corporation of America  
Missile Electronics and Control  
Burlington, Massachusetts

by

Radio Corporation of America  
Electron Tube Division  
Microwave Operations  
Harrison, N. J.



Prime Contract No. AF30 (602) -2115

P. O. No. GX 806067-L61

## TABLE OF CONTENTS

Section	Page
List of Illustrations . . . . .	111
Abstract. . . . .	iv
 I INTRODUCTION. . . . .	 1
I. Purpose. . . . .	1
II. Objective Specifications . . . . .	2
III. General Design Approach. . . . .	3
A. Modification of the Basic Type 6861 Design. . . . .	3
B. Development of a New Helical-Coupled Traveling-Wave Tube . . . . .	 3
C. Plan for this Program . . . . .	6
 II THEORETICAL NOISE STUDIES . . . . .	 7
I. Noise-Reduction Regions. . . . .	7
II. The Low-Noise Cathode. . . . .	10
III. Noise Reduction in the Cathode-Anode Region. . . . .	12
A. Reduction in Kinetic Voltage Fluctuations . . . . .	14
B. Correlation Effects in a Low-Velocity Electron Stream . . . . .	 29
C. Noise-Shielding Effects of a Very Dense Space Charge Cushion. . . . .	 33
IV. The Transformer or Impedance Matching Section. . . . .	37
V. RF Transducer Section and Interaction Region . . . . .	38
 III EMPIRICAL RESULTS . . . . .	 41
I. Preliminary Tests and Evaluations. . . . .	41
A. Development of the RCA Low-Noise Electron Gun . . . . .	 41
B. The Basic Type 6861 Low-Noise Gun Design. . . . .	44
C. Summary of Preliminary Experimental Results . . . . .	57
II. New Low-Noise Electron Gun Designs . . . . .	59
A. Modified 6861 Electron Gun Design . . . . .	59
B. Created Space Charge Electron Gun Design. . . . .	61
C. Electron Gun Evaluation Plans . . . . .	62
III. Solenoid Focusing Methods. . . . .	63
 IV CONCLUSIONS . . . . .	 67
 V PROGRAM FOR NEXT INTERVAL . . . . .	 68
 APPENDIX A NOISE-FIGURE MEASUREMENTS . . . . .	 69

# LIST OF ILLUSTRATIONS

Figure		Page
1	Cross section of the type 6861 "bottle". . . . .	4
2	The four main functional areas in low-noise electron gun design. . . . .	9
3	Electron velocity distributions. . . . .	16
4	Angular velocity of an electron moving under the influence of an axial magnetic field and a radial electric field as a function of radius . . . . .	21
5	Noise reduction using cross-field effects to narrow the axial velocity spread of a beam of electrons . . . . .	23
6	Potential distribution in parallel plane diode with finite emission velocity . . . . .	31
7	Theoretical optimum noise figure vs. frequency for various current densities. . . . .	36
8	RCA Type 6861. Noise figure distribution in 88 tubes. .	43
9	Basic features of the RCA Type 6861 low-noise electron gun. . . . .	45
10	RCA Type 6861. Noise-figure variation with tube parameter adjustment . . . . .	47
11	Experimental tube-noise figure results with modified type 6861 and other tube designs . . . . .	49
12	Cyclic behavior of noise figure vs. magnetic field for type 6861 in which launching angle ( $\phi$ ) is relatively large. . . . .	50
13	Beam launching characteristics of a single RCA Type 6861 tube (Ser. No. 179) . . . . .	52
14	Beam edge potential profile of a single RCA Type 6861 tube (Ser. No. 179). . . . .	53
15	Effects of Einzel-Lens type impedance transformation on tube noise figure in the basic type 6861 design . . .	55

## LIST OF ILLUSTRATIONS

Figure		Page
16	Approximate beam edge potential profile for modified multigrid 6861 tube design. . . . .	56
17	RCA Type 6861. Gain, power output, and noise figure under fully optimum conditions. . . . .	58
18	Proposed structure for ultra-low-noise electron gun -- Design A. . . . .	60
19	Proposed structure for ultra-low-noise electron gun -- Design B. . . . .	62
20	Proposed scheme for initial focusing package. . . . .	65
21	Tapered field solenoid characteristics. . . . .	66
22	Block diagram of noise-figure measurement setup . . . .	71

ABSTRACT

→ A description is presented of

This report describes the early stages in the development of a very low noise traveling-wave tube, designed for operation at S-band frequencies. The tube is to have a minimum gain of 25 db and a maximum tube noise figure of 2 db over the frequency range 2.7 to 3.5 kmc.

Theoretical studies <sup>were</sup> have been made to determine methods of reducing noise in beam-type devices. Attempts were made to correlate some of the experimental low-noise data with the proposed theories. Based on the results of these preliminary studies, the effort during this program will be primarily directed toward improving the noise performance of an existing low-noise tube design, the RCA Type 6861 traveling-wave tube. However, the development of a new, more compact design than that of the 6861 tube will also be considered.

The interim tube requirements are essentially the same as those for the type 6861 except for the much lower noise-figure requirement. Early <sup>were</sup> efforts have been directed toward a general re-evaluation of the 6861 tube design, especially with regard to its noise performance. In addition, improvements in coupling and focusing techniques were ~~also~~ considered.

Preliminary tests <sup>SHOWN</sup> have ~~shown~~ that the prototype <sup>tube</sup> 6861 design, under normal operating conditions, is capable of achieving noise figures as low as 5 to 6 db. This tube, when operated under optimum beam-launching conditions and in a higher magnetic confining field, can have noise figures as low as 3 to 4 db. Cathode improvements are expected to reduce

Cont. on p. VI

the noise figure of this basic design to approximately 2 to 3 db.

Investigations have ~~also~~<sup>SHOWN</sup> shown that a reduction in the noise figure below the 2 to 3 db level requires a redesign of the low-noise electron gun, and several design versions are being considered. The new electron gun design, in conjunction with more efficient couplers and an improved focusing system, is expected to reduce the tube noise figure to the required 1 to 2 db level.

During the next quarter, effort will be expended toward the achievement of the required noise performance with interim tube and solenoid designs.



## SECTION I

### INTRODUCTION

#### I. PURPOSE

Traveling-wave tubes, because of their high gain, stability, and broadband characteristics, are being used, with increasing frequency, as microwave amplifiers. These tubes are especially attractive to system designers, who use the black-box design technique, since they are integral two-terminal devices and require only a conventional-type power supply to form a complete microwave amplifier unit.

Recent advances in the techniques for reducing noise in traveling-wave tubes have greatly enhanced the already outstanding performance capabilities of these tubes, and they are now singled out as the favored input amplifier for use in the UHF through X-band frequency ranges.

This report describes the early stages of the program to develop a very low-noise traveling-wave tube and to demonstrate its operation in the S-band frequency range.

#### II. OBJECTIVE SPECIFICATIONS

The tube developed under this program is intended to operate to the following specifications:

Frequency range	2.7 to 3.5 kmc
Tube noise figure	2 db (maximum)
Small-signal gain	25 db (minimum)

Saturated power output	1 mw (minimum)
Focusing	Solenoid
VSWR of input	2 to 1 (maximum)
VSWR of output	2 to 1 (maximum)

### III. GENERAL DESIGN APPROACH

The development of the proposed traveling-wave tube will rely, to a large extent, upon the theoretical and empirical knowledge gathered by RCA during past development programs and upon RCA's extensive experience in the design and testing of low-noise devices. In addition, the theories and experimental results of other workers in the low-noise field will be used as a guide to determine state-of-the-art attainments and for confirming the improvements that are derived during this program.

At the beginning of this program, a brief feasibility study was made, which indicated that there are two general approaches that can be used to achieve the desired performance characteristics for the proposed traveling-wave tube. First, modifications can be made to the basic RCA Type 6861 traveling-wave tube; second, a new helical-coupled tube design can be developed. These approaches, described briefly in paragraphs A and B below, both require an extensive beam-noise-reduction program and differ only in the construction of their rf circuits.

#### A. Modification of the Basic RCA Type 6861 Design

The basic RCA Type 6861 tube meets all the requirements of the proposed traveling-wave tube except that of tube noise figure. The 6861 tube uses a relatively high-impedance helix, ruggedly supported by three ceramic rods that are firmly clamped at periodic intervals along the helix length. Coaxial-cavity type input and output rf couplers are voltage coupled to antennas that terminate the tube helix. The 6861 design has a very low-loss rf circuit which contributes to the low tube noise figures that have been achieved consistently with this tube. Figure 1 shows a cross section of the "bottle" for the 6861 tube.

Recent evaluation studies have indicated that tube noise figures as low as 3 db can be achieved with the existing design of the 6861 tube, if the magnitudes of the operating voltages and the magnetic focusing field are made optimum. Thus, the 6861 tube could very well serve as the prototype design for the proposed traveling-wave tube, and only an improved low-noise electron gun would be needed in order for this tube to achieve the required low-noise performance. Because of the apparent feasibility and facility of obtaining the desired objectives with a modified 6861 design, the emphasis will be placed on this design approach.

#### B. Development of a New Helical-Coupled Traveling-Wave Tube

In the past, the use of helical rf coupling with low-noise traveling-wave tubes was limited for two reasons. First, the helical couplers caused a much greater signal attenuation than either waveguide or coaxial-cavity couplers; second, an increase in the tube noise figure was expected because the helical couplers do not excite the wave at the beginning of the

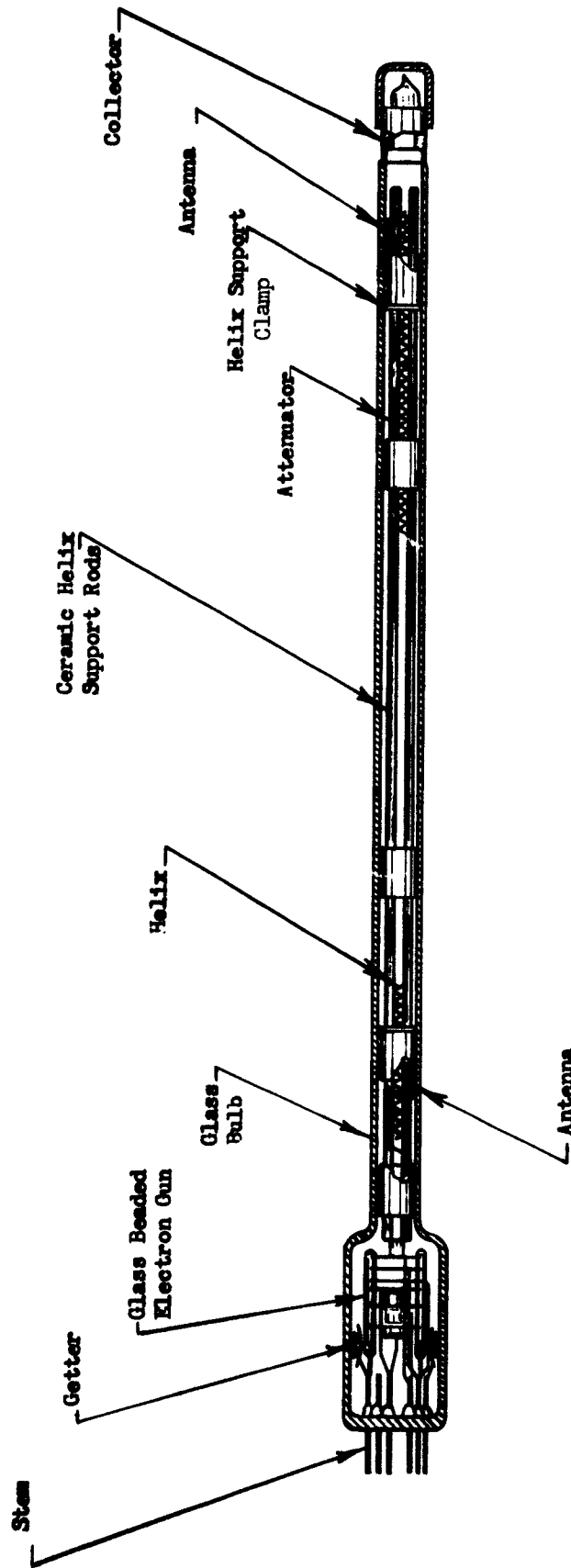


Fig. 1 — Cross section of the type 6861 "bottle".

helix while the beam noise does. However, these difficulties have been minimized by the extensive work, done by the RCA Microwave Design and Development Group, in the development of helical couplers.

As a result of this work, helical couplers have been developed that have coupling losses as low as 0.3 to 0.4 db. These values are about the same as for the normal coaxial-cavity couplers. Also, measurements to determine the extent the noise figure increases when helical coupling is used, indicated that this factor has been over emphasized. The increase in tube noise figure is in the order of 0.1 db, not enough to prohibit the design of a traveling-wave tube which will meet the objective specifications for this program. In addition, the increased circuit losses that results from the use of the small-diameter fluted-glass helix support structure can also be expected to increase the overall tube noise figure about 0.1 db. Thus, the overall increase in tube noise figure that occurs when helical coupling and the fluted-glass support structures are used, would be only about 0.2 to 0.3 db more than that obtained when an equivalent design using a three-rod supported helix and coaxial-cavity couplers is used.

The helical couplers, however, have several decided advantages which outweigh the small increase in terminal noise figure that results from their use. These are:

1. The simplicity of their construction permits the helical couplers to be easily fabricated.
2. When helical couplers are used, the broadband coupling can be easily adjusted.

3. In addition, the smaller physical size of traveling-wave tubes using helical couplers permits the design of smaller, more efficient solenoids and enhances the subsequent possibility of developing a permanent-magnet-focusing package for the traveling-wave tube.

#### C. Plan for this Program

The development work under this program will emphasize a traveling-wave tube design based on the RCA Type 6861 tube, but this design will incorporate a vastly improved low-noise electron gun. However, some exploratory work, comparing the noise performance of a small-diameter helical-coupled tube design with that of a tube using improved coaxial-cavity couplers, is also planned. Solenoid focusing will be used for all the interim tubes developed during this program.

## SECTION II

### THEORETICAL NOISE STUDIES

#### I. NOISE REDUCTION REGIONS

For many years, vigorous attempts have been made to reduce tube noise in an effort to increase receiver sensitivity at microwave frequencies, and for traveling-wave devices (backward-wave and forward-wave amplifiers), considerable progress has been made, and the noise figures of these devices are being steadily reduced. Early in 1956, RCA reported an S-band traveling-wave amplifier with a tube noise figure as low as 4.8 db.<sup>1</sup> Shortly thereafter, the noise figure was reduced to approximately 4.1 db. At that time, the excellent empirical results, being obtained by RCA, forced a revision in the noise theory to permit the prediction of the low noise figures that were being achieved. Subsequently, the state of the art was successfully advanced, and even greater noise-figure reduction has been achieved. Recent work at RCA has resulted in the development of S-band traveling-wave tubes with tube noise figures as low as 3.2 db. Also, Currie<sup>2</sup> has reported the attainment of a 3 db noise figure for a backward-wave amplifier operated at 2.6 kmc and Watkins indicated that noise figures of 2 to 3 db could be achieved for L-band traveling-wave devices.

1. E.W. Kinaman, M. Magid, "Very Low Noise Traveling-Wave Tubes, Presented at the Second Annual Meeting on Electron Devices, October 1958.

2. M.R. Currie, D.C. Forster, J. Appl. Physics 30, 94, 1959.

The problems that must be solved, in the development of low-noise traveling-wave tubes, are many and diverse. Practical solutions to many of these problems are well known, and the extension of the noise theory has indicated a number of other techniques that may be employed to effect even greater noise reductions.

For purposes of this discussion, the factors vital to the attainment of low-noise performance in traveling-wave tubes are separated into four distinct regions of the tube structure. These four regions are listed below, and Fig. 2 shows their functional relationship.

1. The cathode region. The nature of the cathode is a prime factor in the determination of the noise figure of a traveling-wave tube.
2. The cathode-anode, or beam-launching, region. This is the region at the front of the cathode emitting surface. In this region, the fluctuations in electron velocities can be comparable in magnitude to the average electron velocity.
3. The transformer, or impedance-transformation, region. This extends approximately from the end of the cathode anode region to the plane of the circuit input. In this region, the fluctuations in electron velocities are usually small compared to the average electron velocity.
4. The interaction, or rf circuit, region. This region lies between the circuit-input and circuit-output planes.

The effects on tube noise performance of the cathode region, the impedance-transformation region, and the interaction region are relatively



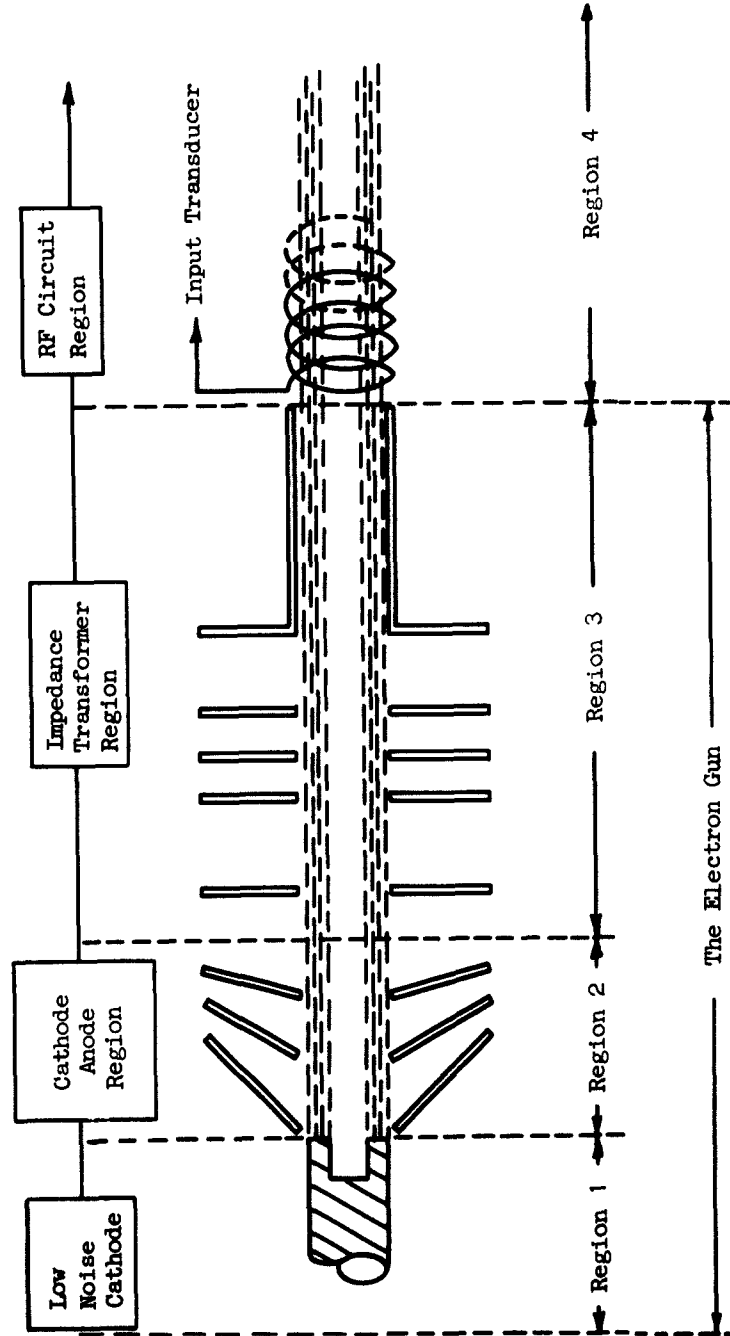


Fig. 2 — The four main functional areas in low-noise electron gun design.

well known, and these effects have long been exploited in the design of low-noise traveling-wave tubes. The effects of the beam-launching region on tube noise performance are not as familiar as are the effects of the other regions; however, theoretical and experimental analyses of this region have demonstrated that it has a tremendous effect on the noise performance of the traveling-wave tube. A full utilization of the techniques of noise reduction, in each of the four regions, is required to achieve a maximum tube noise figure of 2 db over the frequency range 2.7 to 3.7 kmc.

The importance and theoretical and empirical significance of each of the four noise-reduction regions, in obtaining solutions to the basic noise problems, are discussed in paragraphs II through V of this section.

## II. THE LOW-NOISE CATHODE

The minimum tube noise figure that can be achieved is not limited by the electron gun design and circuit parameters alone, but it is also a function of the nature of the electron emitter. The characteristics of the cathode that effect noise performance are, therefore, of prime importance.

The idealized one-dimensional single-velocity noise-figure theory predicts a minimum noise figure of about 6 db for a beam-type microwave amplifier. This minimum is based upon the assumptions that (1) the noise at the potential minimum is given by uncorrelated shot-noise current and Rack velocity fluctuations;<sup>3</sup> and (2) no noise-reduction mechanisms are present. In addition, this theory assumes that the cathode is uniform

3. A.J. Rack, "Effects of space charge and transit time on shot noise from diodes," Bell System, Tech. J., Vol. 17, pp. 592-619, October 1938.

in every respect, in which case, the current density fluctuations and velocity fluctuations are everywhere similar. While these conditions may be approximated in the ideal low-noise cathode, in practical cathodes, the emission density and velocity distribution may vary from point to point over the cathode for a number of reasons. W. R. Beam<sup>4</sup>, formerly of the RCA Laboratories at Princeton, has shown that a high noise figure, in an otherwise low-noise tube design, is almost certainly due to excessive noise velocity, brought about by cathode nonuniformities. This contention has been supported by the experimental data gathered in the low-noise work performed by the RCA Microwave Design and Development Engineering Group at Harrison, N. J. Tube noise-figure increases of up to the order of 3 db (total beam noise power doubled), which could be attributed to cathode emission defects, have, in fact, often been observed. Usually, these noisy cathodes were fluffy, rough, uneven, and/or partially sintered, compared to the smooth, dense homogeneous coating of the normal low-noise cathode.

In general, there are four cathode features which have pronounced effects on tube noise characteristics. These are:

1. The nature of the cathode base metal
2. The nature of the cathode coating
3. The cathode activation procedure
4. The cathode operating temperature

The cathode base metal is important because it is a major factor in determining the nature of the interface between the oxide coating and the

---

4. W.R. Beam, "Noise wave excitation at the cathode of a microwave beam amplifier," I.R.E. Transactions on Electron Devices, Vol. ED-4, No..3; July 1957

metal base during both the cathode's activation and its eventual operation as an electron emitting device. Increased noise may occur, due to the effect of the cathode interface on the oxide deposit, and this has been observed in some tubes.

Low-noise cathodes are usually coated with a dense, homogeneous deposit of emitting material, which has a thickness in the order of 0.007 to 0.0012 inch. Spray techniques are adjusted to provide the desired emitter coating, and meticulous care must be taken to protect the coating during tube sealing. Low tube pressures and cathode temperatures must be maintained during every phase of tube degassing and activation, in order to develop the final active cathode surface without materially changing the original sprayed condition. With proper activation, such a coating provides adequate uniform emission at temperatures as low as 600°C to 650°C.

The successful application of low-noise cathode processing techniques results in a high-emission, long-life source of electrons and in a minimum of the noise that can be attributed to defects in the cathode volume or interface region. RCA test data indicates that the life of the type 6861 tube usually ranges between 10,000 and 20,000 hours. This life characteristic has been confirmed by reports from users of the type 6861 tube in a number of applications.<sup>5</sup>

### III. NOISE REDUCTION IN THE CATHODE-ANODE REGION

The very low noise figures, which have been recently observed in traveling-wave tubes, has led to a re-examination of possible noise-

5. It has been reported that the type 6861 tube operated satisfactorily for 19,800 hours in radar equipment at the Zurich Airport, Switzerland.

reduction mechanisms. In particular, the single-velocity approximation has been proved invalid, when applied in the low-velocity, space-charge-depressed cathode region. The reduced noise figures that have been observed in this region are now attributed, in part, to the fact that initially uncorrelated fluctuations may become partially correlated while being propagated along a multivelocity electron beam.<sup>6</sup> Data compiled by the RCA Microwave Design and Development Group also indicated that some noise reduction is effected by mechanisms which reduce the axially directed velocity fluctuations in the electron stream.

More recent experiments, however, indicate that the current density in the region of the cathode is a more critical factor in the attainment of greater noise reduction. Also, theoretical studies by Berghammer and Bloom,<sup>7</sup> at RCA, indicate that the action of a very dense space-charge cushion, immediately in front of the cathode, could produce a noise shielding effect.

Thus far, widely divergent theoretical explanations have been given of the necessary and most favorable conditions for low-noise operation in the cathode-anode region. From these explanations, one factor is conclusively indicated -- a low potential, long-drift region is definitely needed to effect a high measure of noise reduction. Results of studies by the RCA Microwave Design and Development Group indicate that, in the cathode-anode region, noise-reduction techniques will fall into three general categories:

6. A.L. Siegman, D.A. Watkins, A.C. Hsieh, "Density-Function Calculations of Noise Propagation in an Accelerated Multivelocity Electron Beam," *Journal of Applied Physics*, 29, 1138, 1957.

7. J. Berghammer, S. Bloom, "A Microscopic Analysis of Velocity-Spread," *Sixth Annual Conference on Electron Tube Research*, Quebec, June 1959.

1. The techniques used to reduce kinetic voltage fluctuations.
2. The techniques devised for reducing noise current fluctuations.
3. The techniques required to establish correlation effects between the current and voltage fluctuations.

Studies have also indicated that the beam-launching methods required to accomplish noise reduction, in each category, are quite similar, and it may be difficult to ascertain, from experimental data alone, in which category the noise reduction is achieved. In fact, the possibility exists that noise reduction may be simultaneously achieved in all three categories in a particular tube design. This possibility is discussed, in more detail, in a subsequent paragraph.

#### A. Reduction in Kinetic Voltage Fluctuations.

When the low-noise cathode is operated under temperature-limited conditions, the noise factors in the electron beam consist of a noise current, which is pure shot noise, and a noise velocity fluctuation, which is the deviation of the electron velocities from the mean electron velocity, as described by the Maxwellian distribution of electron velocities.

When the low-noise cathode is operated under space-charge-limited conditions, the noise current is modified by the action of the potential minimum. However, since the average electron velocity is not affected by fluctuation of the potential minimum, there can be no change in the velocity fluctuations in the electron stream. Velocity fluctuations are statistically independent, or invariant, if no energy exchange occurs within the electron stream. Therefore, any reduction in the kinetic voltage

fluctuations implicitly expresses either a redistribution of electron velocities or a loss of energy within the electron stream.

The kinetic voltage is determined by the amount of electron-velocity deviation from the mean value of emission velocities; therefore, in order to reduce the kinetic voltage, the thermal velocity spread must be reduced. The velocity-spread effect is illustrated in Fig. 3. The distribution in the velocities of electrons emitted from the ideal low-noise cathode will very closely follow the normal Maxwellian distribution at the potential minimum, as indicated by curve A, Fig. 3; but the practical cathode probably generates a distribution containing an increased number of higher-velocity components, as shown in curve B. These higher-velocity components are primarily due to the granular nature of the cathode deposit.

If the axial velocity spread (primarily the higher-velocity components) can be reduced as shown in curve C, then the kinetic-voltage fluctuations will have been reduced, and the electron beam noise will be below that which normally corresponds to the cathode operating temperature -- that is, the electron gas will have been "cooled".

Two possible methods of reducing kinetic voltage fluctuations are discussed below. The first method involves electric fields only; the second, crossed electric and magnetic fields.

1. Electrostatic Method of Velocity-Spread Reduction. -- The electrostatic method of reducing the electron velocity spread utilizes the chromatic-aberration defect of electron lenses. Stated simply, the

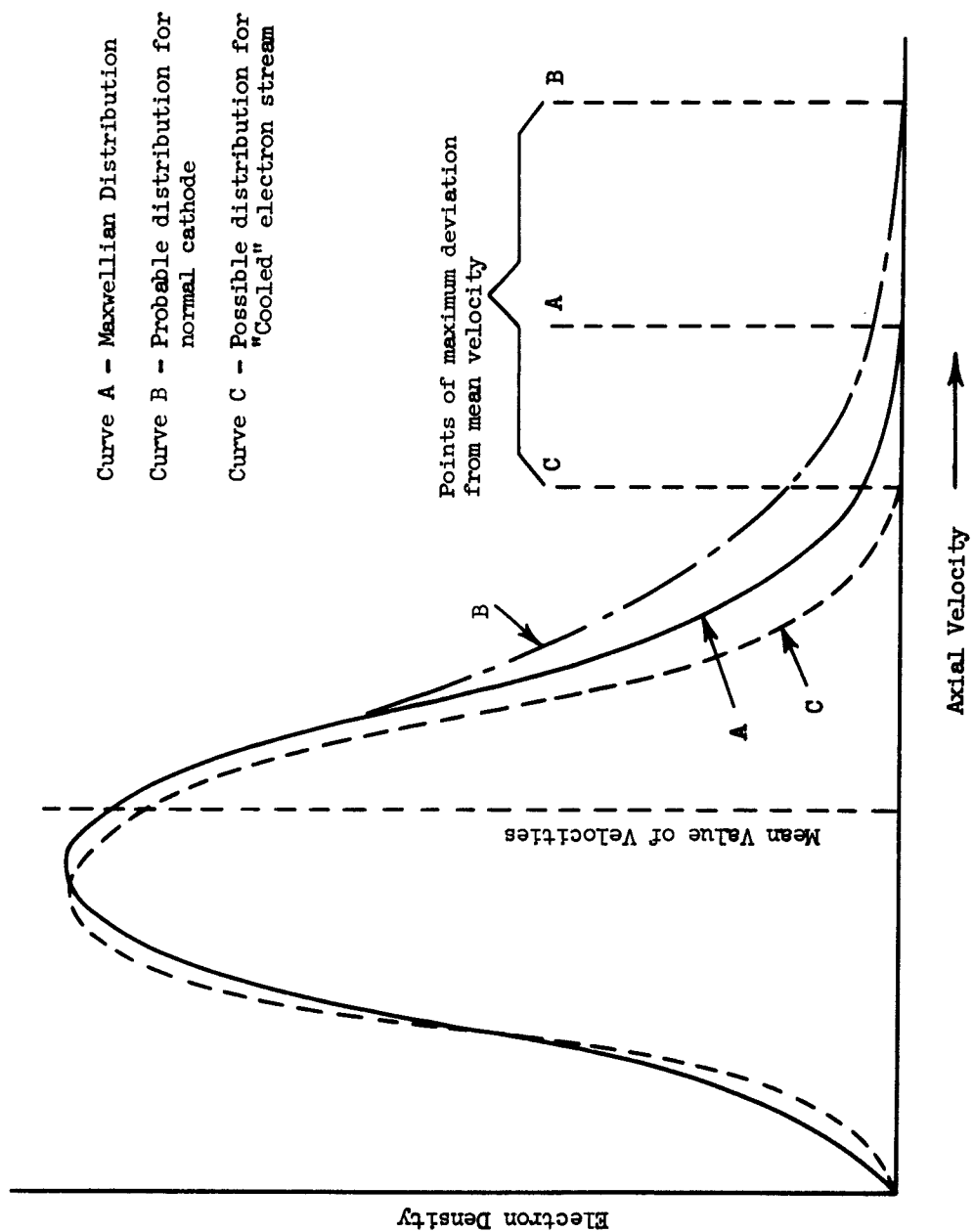


Fig. 3 - Electron velocity distributions.



chromatic aberrations in the electron lens system reduce the axial velocity spread in the image below that of the object by a process analogous of the chromatic dispersion effects in optics.

Although chromatic-aberration effects exist in all positive (converging) electrostatic lenses, the Einzel-type lens is preferred. The Einzel-lens formation begins and ends at the same potential value; therefore, it may be placed anywhere in the electron stream without disturbing adjacent potential relationships.

Since the converging effects in the Einzel lens are stronger than the diverging effects, this lens exhibits a converging action regardless of whether the center electrode is more positive or less positive than the outer electrodes. Therefore, in a simple analysis, the Einzel lens can be considered as an equivalent single-aperture electrostatic lens, and considering only first order effects, the focal length of the lens is given by the relation,

$$f = \frac{4V}{V_1' - V_2'} \quad (1)$$

where  $f$  is the relative focal length and  $V$  is the potential along the axis. If the different electrons have energies corresponding to the different values of  $V$  then,

$$\frac{df}{dV} = \frac{f}{V} \quad (2)$$

Equation (2) infers that the focal length is dependent upon the electron energy, in that, the greater the energy (electron velocity), the smaller is the change in focal length. Thus, the axial velocity spread in the electron stream at the focus is narrowed by the foreshortening of the electron paths as a function of electron velocity. The physical explanation of this relationship is that this type aberration results from the fact that, in the electrostatic lenses, the higher-velocity electrons spend a proportionately longer time in the retarding fields of the lens than they do in the accelerating fields.

In practice, an Einzel-type lens can be established, in the cathode-anode region, by means of a system of closely spaced apertures or, in the cathode region, through the use of a beam-shaping element, which works in conjunction with the anode to determine the electric field configuration. A strong magnetic field is used to confine the electron stream to a desired path and to maintain a high-density space charge.

The application of the Einzel lens noise-reduction technique, to the cathode-anode region, results in the establishment of a virtual cathode image, beyond the potential minimum, in which the spread in axial velocities in the electron stream has been substantially reduced over that present in the object (potential minimum). The cathode image is now used as the reference plane for the transformation of noise-space-charge waves to the desired beam impedance at the helix input. Another factor of importance is that the Einzel-lens technique could be applied, a second time, to the impedance-transformation region of the low-noise

gun, and an even greater reduction in the velocity spread and a further reduction in beam noise may possibly be achieved in this way. This technique is discussed in Section III, paragraphs I and II, of this report.

2. Crossed-Field Method of Velocity Spread Reduction. -- The crossed-field mechanisms for reducing the velocity spread in the electron stream involve the motions of a thin, cylindrical, hollow electron beam in immersed laminar flow, such as that considered by Brewer.<sup>8</sup> Two types of crossed-field noise reduction mechanisms are discussed below:

a. Velocity Exchange Mechanism. -- The equation of motion of an electron beam in immersed laminar flow is given, in cylindrical coordinates, by the expression

$$\ddot{r} - r\dot{\theta}^2 = -\eta E_r - \eta_r \theta B \quad (3)$$

The equation of the angular velocity, when the initial angular velocity is zero, is determined from Busch's theorem to be

$$\dot{\theta} = \frac{\eta}{2\pi r^2} (\phi - \phi_c) = \frac{\eta B}{2} \left[ 1 - \left( \frac{r_c}{r} \right)^2 \right] \quad (4)$$

where B represents the magnitude of the uniform magnetic field in which the emitting surface and the electron beam are immersed;  $r_c$  is the radius at which the electron leaves the emitting surface;  $\phi_c$  is the total flux

8. G.R. Brewer, "Some characteristics of a cylindrical electron stream in immersed flow," IRE Transactions on Electron Devices, Vol. ED-4, No. 2, April 1957.

threading the cathode out to radius  $r_c$ ; and  $\eta$  is the charge-to-mass ratio for the electron. Equation (4) defines the motion of an electron beam in immersed flow.

Consider the conditions where electrons, originating from a point on radius  $r_c$ , are allowed to expand (diverge). Equation (4) shows that such an expansion of the mean beam radius requires that the electrons possess a mean rotational (precessional) angular velocity around the beam axis, as given by the expression

$$\dot{\theta}_{\text{avg.}} = \frac{\eta B}{2} \left[ 1 - \left( \frac{r_c}{r} \right)^2 \right] \quad (5)$$

where  $r$  is the expanded mean radius. Equation (5) indicates that the angle of precession,  $\theta$ , at some given reference plane, determined by a transit time  $t$ , depends upon the magnetic field  $B$  and the factor

$$1 - \left( \frac{r_c}{r} \right)^2$$

Thus, for a given magnetic field,  $B$ , the precessional angular velocity will vary from zero, when  $r$  is equal to  $r_c$  (no divergence), to the velocity that corresponds to the Larmor frequency, when  $r$  becomes large compared to  $r_c$ . More specifically, the precessional angular velocity is a power function, and as shown in Fig. 4, it increases rapidly for small increases in beam expansion.

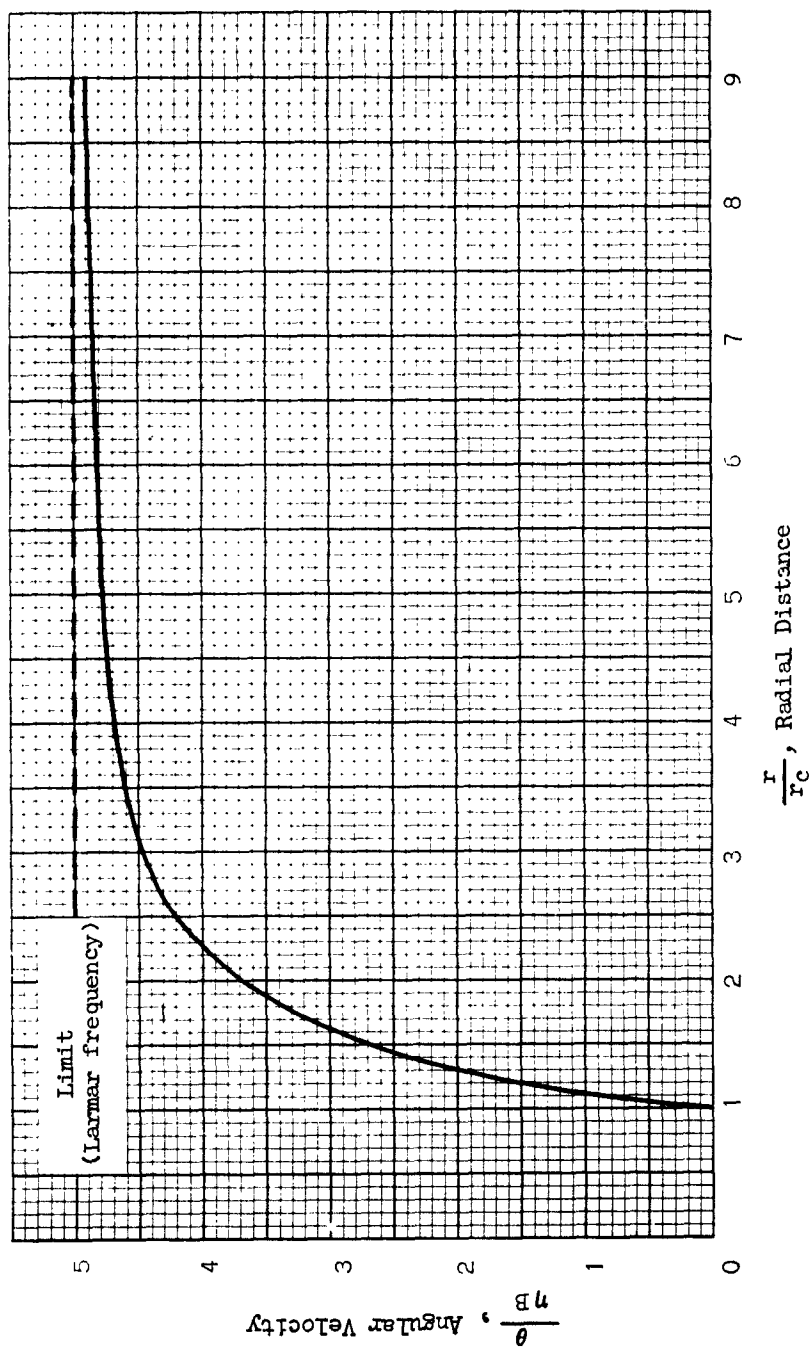
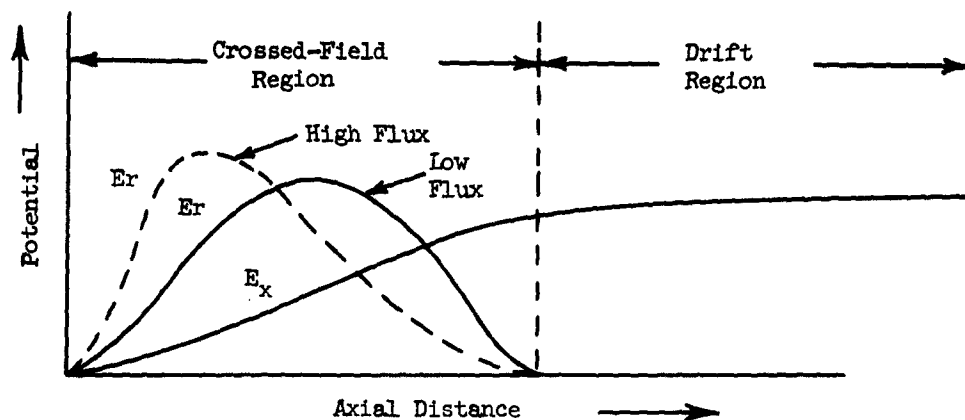


Fig. 4 — Angular velocity of an electron moving under the influence of an axial magnetic field and a radial electric field as a function of radius.

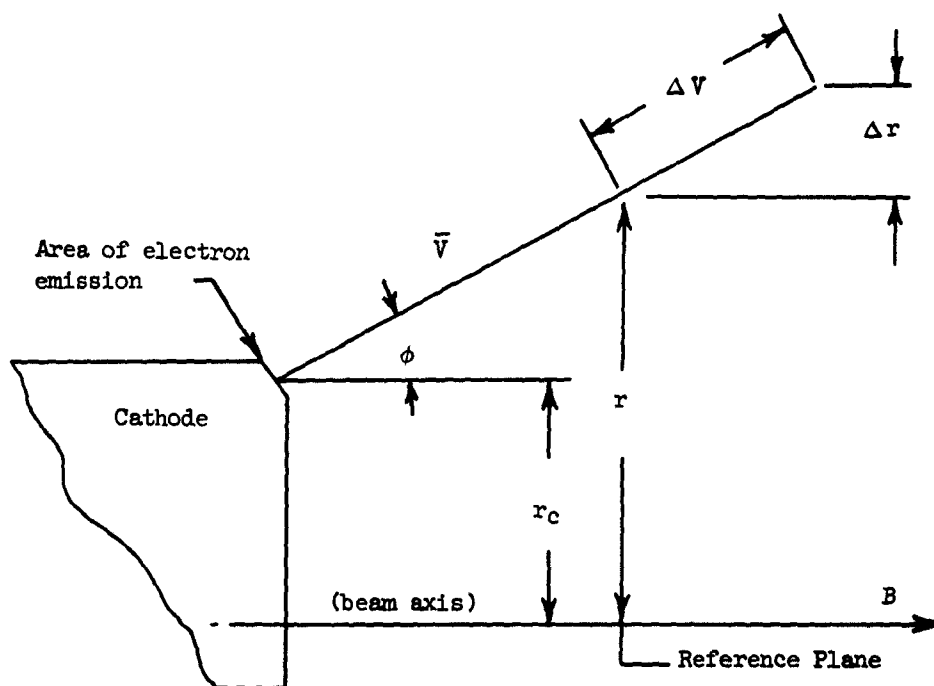
This property of the electron beam in immersed flow may be a useful mechanism for reducing the electron-beam velocity spread. For example, consider a thin annular beam of radius  $r_0$ , expanded in a two-dimensional electric field to a mean radius  $r$ , as shown in Fig. 5. Assume that the magnetic field  $B$  is of sufficient strength to prevent the crossing of electron trajectories at the cathode. If this condition exists, the electrons are then launched at some fixed angle  $\phi$  with respect to the beam axis. At the reference plane, the beam expands to a new mean radius,  $r$ , determined by both the maximum radial component of the electric field and the radial component of the mean thermal velocity. The constraining magnetic field  $B$  will then cause the electrons to actually precess around the axis of the electron stream at a velocity determined by the relationship expressed in equation (5).

Since the velocities of most of the electrons in the stream will be in the narrow classes of velocities situated about the mean velocity (see Fig. 3), the main stream of electrons will precess with an average velocity determined by the average beam radius and the magnetic field  $B$ .

Now consider the motions of electrons that move at velocities much greater than the mean velocity of the electron stream. The initial energies of these higher-velocity electrons are greater than that of electrons moving at the mean velocity; therefore they will assume radii of excursions, depending upon their initial thermal energies, that are proportionately larger than the mean excursion radius. However, according



(a) Two-dimensional electrical fields possible at cathode-anode region.



(b) Launching Conditions

Fig. 5 — Noise reduction using cross-field effects to narrow the axial velocity spread of a beam of electrons.

to equation (5) and as shown graphically in Fig. 4, a linear expansion in radius is accompanied by a very rapid, compensating increase in precessional angular velocity. Thus, the greater the expansion -- i.e., the greater the thermal velocity -- the greater the precession rate ( $\theta$ ) becomes.

In the region near the potential minimum ( $\alpha$  region), the effects of the two-dimensional electric field can cause the fluctuations in thermal velocities to be of the same order of magnitude as the average velocity of the electron stream. Therefore, electron excursions that are a function of the thermal velocity can produce appreciable effects on the noise performance of the traveling-wave tube. For example, under highly divergent (large launching angle  $\phi$ ) conditions, the electrons with the highest thermal components can easily have excursion radii 10 to 30 per cent larger than electrons moving at the mean thermal velocity. Thus, under these conditions, the angular velocity,  $\theta$  can increase in the order of 5 to 10 times.

It appears that the higher-velocity electrons, by precessing faster, must, under conditions of a strong constraining magnetic field, move across the main electron stream, which precesses at a lower velocity. Therefore, there is a finite probability of some velocity exchange between the higher-velocity electrons and the main electron stream, and the amount of this exchange is proportional to the difference in their precessional velocities. In addition, the probability of an energy exchange, as a result of electron-electron or electron-ion collisions, also exists as a strong function of the charge density. The net result of these mechanisms



could be a general redistribution of the electron velocities into a narrower range of velocities, as shown by curve C, Fig. 3. More important, the high-velocity components, which are the major noise producers in the electron stream, could be effectively reduced. An important factor to be remembered is that, if any energy exchanges do take place, the kinetic voltage fluctuations are no longer invariant in this region.

The launching angle  $\phi$  (see Fig. 5(b)), not only determines the instantaneous spread of the electron excursions ( $\Delta r$ ) that results from different thermal velocities but also, in conjunction with the magnetic field  $B$ , determines where in the gun region the cathode image will occur -- i.e., where the beam becomes focused. It is easily shown that focusing occurs when the electrons have precessed  $2\pi$  radians during their transit from the cathode to this focus plane. If the current density is constant and the launching angle fixed, the focusing will occur in the focus reference plane whenever the magnetic field strength is increased in even multiples over that which caused the first precession of  $2\pi$  radians.

However, for a precession of just  $2\pi$  radians to occur at the fixed focus plane, any increase in the magnetic field requires that the launching angle  $\phi$  be also increased. Thus, increasing magnetic fields require an increasingly transverse component of the electric field off the cathode. This is also a necessary condition for the formation of a low-velocity electron stream in which correlation effects between noise current fluctuations and kinetic voltage fluctuations are believed possible.

In addition, these same conditions can result in an electric field configuration which is essentially that of the Einzel lens discussed previously.

If the electric field gradient, which caused the original divergence of the electron beam, is now removed, and the cooler electron stream is allowed to drift, then the smoothing effects of the space charge, the high magnetic flux, and possible bunching effects in the electron stream could result in a further noise reduction in the drift region. In this way, the emission noise that results from the high-electron-velocity components, can be substantially reduced at some particular reference point. The impedance at this reference point is then transformed by the exponential-transformer or Einzel-lens transformation method to that impedance required at the helix input.

The techniques discussed above, although important noise-reducing schemes, may produce only second order effects compared to methods wherein space-charge forces can play an important part.

b. Energy Exchange Mechanism. -- The divergent beam-launching characteristics of a two-dimensional electric field (see Fig. 5) is an effective mechanism for converting a portion of the potential axial velocity fluctuations into radial velocity fluctuations (transverse space-charge waves). As shown in Fig. 5, the displacement of groups of electrons ( $\Delta r$ ), due to their thermal velocities, results in a net charge density, which produces an electrostatic field such that

$$E = 4\pi ne (\Delta r), \quad (6)$$

where  $e$  represents the charge of the electron,  $n$  is the number of electrons displaced, and  $r$  is the amount of electron displacement in the radial direction. Since the restoring force on an electron of mass  $m$  is  $eE$ , then, the equation for the electron motion is

$$m\ddot{r} - 4\pi n e^2 (\Delta r) = 0, \quad (7)$$

where  $\ddot{r}$  is the acceleration of the electrons in the radial direction. Essentially, this is the equation for the simple harmonic motion of the electrons that are displaced, by some means, in a plasma.

Figure 5 (a) shows the variations of the radial field component ( $E_r$ ) of the electric field in the cathode region. This component exists for only a short distance, building up from zero at the cathode to a maximum and then falling off to zero again.

The  $E_r$  component primarily determines the launching angle  $\phi$ , and the displacement component  $\Delta r$  is primarily determined by the thermal velocity. Thus, forces disturbing electron oscillations in the transverse direction are thermal velocity components; therefore, the amount of disturbance (electron excursions) is directly dependent upon the initial thermal velocities of the electrons.

When the  $E_r$  component is in the correct relationship to the constraining magnetic field  $B$ , it is possible for the displaced electrons to give up energy to the radial field during that portion of the oscillatory cycle that the electrons are returning to the beam axis.

However, by the time the electrons have completed their dispersive half of the oscillatory cycle and are ready to move away from the beam axis, the  $E_r$  field decays. This should prevent the  $E_r$  field from ever imparting energy back to the electrons. Therefore, there is a net loss of energy by the displaced electrons; this energy loss is proportional to the initial thermal velocities of the electrons. Thus, this mechanism would reflect in a reduction in the axial velocity spread of the electron beam in the drift region (see Fig. 5) compared to that at the potential minimum; and by reducing this axial velocity spread, a reduction in beam noise is achieved.

The process may also be visualized by considering that expansion of the higher-velocity electrons, moving in the positive radial direction, results in the conversion of translational kinetic energy to rotational kinetic energy -- expressed previously, as the precessional motion of the electron stream. However, when the expanded electrons return (due to the effect of electric field forces), the resulting forces on the electrons are now in a direction opposed to the precessional motion, thereby, slowing the rotation. In this way, the kinetic energy of the beam is converted back into potential energy. If at this time, the electric fields, except for a small axial component in the drift field, are removed, and if the electrons are constrained by a strong magnetic field, this could result in a net loss of energy by the expanded electrons. As shown previously, this loss is proportional to the thermal velocity, with the higher-velocity electrons losing more energy to the field than electrons moving at the mean velocity. As a result, the

velocity spread of the axially directed electrons is reduced, and, thus, so is the noise in the electron beam.

One point that should be emphasized again is that, whenever such irreversible energy exchanges occur, the kinetic voltage fluctuations are not invariant in this region.

#### B. Correlation Effects in a Low-Velocity Electron Stream

The analysis of reduced shot noise that occurs with the multivelocitv flow, encountered in space-charge-limited diodes when the transit time is short compared to the rf cycle, has been treated by many workers in the low-noise field. Briefly, the noise reduction is the result of the gating action of the potential minimum; this gating action reduces the noise below the level of pure shot noise in the manner described below.

When a surplus burst of electrons that have velocities sufficient to pass through the potential minimum is emitted from the cathode, the increased space charge which results, causes the potential minimum to become more negative. The more negative potential minimum turns back electrons of lower velocities, which would have normally been able to pass through the potential minimum. However, when higher-velocity electron bursts do not appear, the potential minimum becomes less negative, and an additional number of lower-velocity electrons will pass through the barrier established by the potential minimum. Thus, for every burst of electrons that tends to increase the noise current, there is a compensating current, in the opposite direction, which tends to cancel the noise generated by the electron burst. The result is that the noise current is

smoothed and a noise reduction is obtained which is significantly greater than that which can be achieved under temperature-limited conditions.

Until recently, there was no adequate treatment of emission noise at high frequencies when the transit time is relatively long. Many of the previous analyses of the high-frequency noise problem were based on the single-velocity approximation theory. It was assumed that near the potential minimum, the average velocity was zero, and, therefore, fluctuations in current densities at this point had no effect at a later point in the electron stream. However, it has since been shown that the average velocity at the potential minimum is finite, and thus, there are still current fluctuations at the potential minimum which must also be considered.

The potential distribution in a diode is somewhat as pictured in Fig. 6. The thermal energy of the electrons at the cathode surface imparts initial velocities to the electrons which are distributed according to Maxwell's law. This multivelocity electron flow results in a negative-potential gradient (due to space charge effects) which reaches a minimum at  $X_m$  and has a potential  $V_m$ . A reference plane, termed the  $\alpha$  plane is also shown in Fig. 6. This plane is defined as that point beyond the potential minimum where the spread in velocities between electrons is small compared to the average velocity.

Beyond the  $\alpha$  plane, the single-velocity noise theory again becomes valid. However, in a high-frequency diode, noise determination requires a knowledge of noise current, noise velocity, and of the correlation between

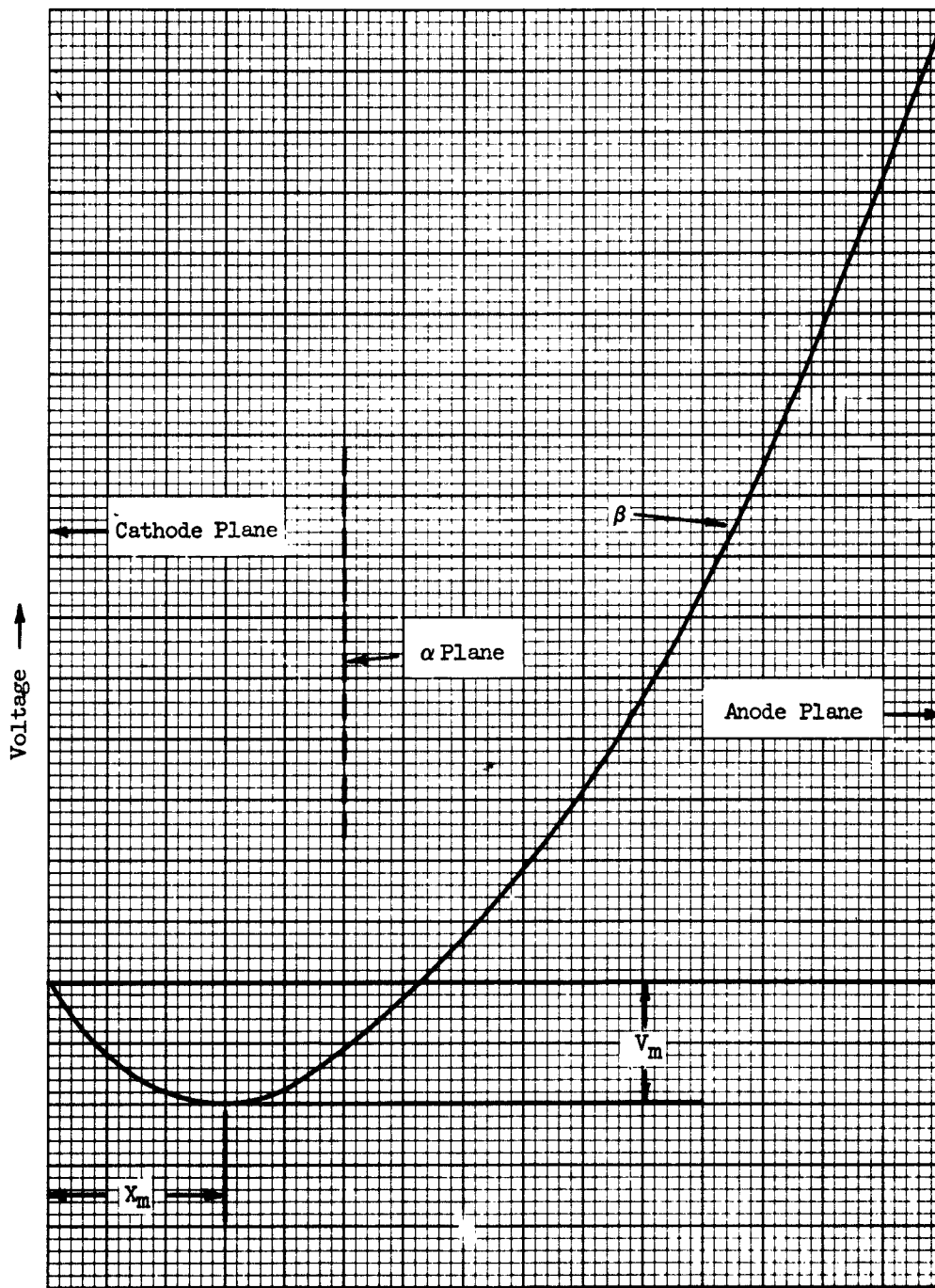


Fig. 6 — Potential distribution in parallel plane diode with finite emission velocity.

these factors in the region between the potential minimum and the plane. According to Tien and Moshman,<sup>9</sup> the noise current, at the plane  $X = 1.2X_m$ , is a strong function of frequency with an almost complete compensation of the disturbing pulse occurring at low frequencies (below 2.5 kmc) and insufficient or over compensation, at the higher frequencies. The RCA Microwave Design and Development Group, at Harrison, N. J. has found some evidence of this type of behavior in low-noise work at L-band, S-band, and C-band frequencies. Later work, by Siegman, Watkins, and Hsieh,<sup>10</sup> predicts that some correlation is introduced in the multivelocity beam as it drifts between the  $1.2X_m$  plane and the  $\alpha$  plane.

Recent low-noise studies have been concentrated upon the region between the potential minimum and the  $\alpha$  plane, where the multivelocity character of the beam is comparable in magnitude to the average velocity of the beam. It will be shown in a later section of this report, that work by the RCA Microwave Design and Development Group has indicated the occurrence of a monotonic decrease in beam noise with an increasing magnetic field (up to field strength of about 1200 gauss) for the type 6861 design. However, along with the increase in magnetic field, there was a progressive decrease in axial beam potential as the electrostatic field configuration was made increasingly divergent, or two-dimensional. While this was done primarily because of the crossed-field requirements, it also greatly extended the low-velocity accelerating region off the potential minimum. Just how much noise reduction can be attributed to

9. P.K. Tien and J. Moshman, "Monte Carlo Calculation of Noise Near the Potential Minimum of a High-Frequency Diode", Journal of Applied Physics, Vol. 27, 1067, 1956.

10. Siegman, et al, op. cit.



crossed-field effects, as described in the previous section, and how much to correlation effects in this drifting region is yet to be determined. What is more important, at present, is that both effects require, in general, the same beam-launching conditions.

Other workers in the field report similar behavior. Foremost among these is the work reported by Currie and Forster<sup>11</sup> in which prime emphasis was placed on the correlation effects in this drift region. This region promises further noise-reduction possibilities when the nature of the mechanism in this region is better understood. It is not known, at present, just how this region affects the noise parameters. There are some indications that the noise-factor reduction in this region may be the result of some finite correlation effects between the voltage and current fluctuations that are generated by the very high velocity components of emission bursts. The gassy nature of the electron beam, under such conditions (due to the high space-charge density and relatively low drift velocity), offers a much greater opportunity for the existence of smoothing effects than that found in the normal (Fry-Langmuir potential distribution) accelerating regions. Much more work is required in the analysis of this region.

#### C. Noise-Shielding Effects of a Very Dense Space-Charge Cushion

Theoretical work by Berghammer and Bloom,<sup>12</sup> at the RCA Princeton Laboratories indicated that the action of a very dense space-charge cushion, immediately in front of the cathode, could produce a noise-shielding effect.

11. M.R. Currie and D.C. Forster, loc. cit.

12. Berghammer and Bloom, op. cit.

To realize this shielding effect, the mean velocity of electron beam drift must be small compared to the thermal velocity over a distance, approximately equal to the Debye length. The Debye length is shown by Berghammer to be:

$$h_o = \frac{1}{\omega_p} \left( \frac{3kT_o}{m} \right)^{1/2} \quad (8)$$

where

$k$  = Planck's constant

$T_o$  = Temperature in degrees Kelvin

$m$  = mass of the electron

Moreover, Spitzer<sup>13</sup> has shown that, for the stationary cloud of electrons, the plasma frequency is related to the frequency of the noise wave by the following dispersion equation:

$$v^2 = \frac{\omega^2}{\beta^2} = \frac{\omega_p^2}{\beta^2} + \frac{3kT_o}{m} \quad (9)$$

where  $\beta$  is the phase constant

This dispersion relationship corresponds to that of a high-pass filter, where the cut-off frequency is equal to the plasma frequency. Thus, noise frequencies below the plasma frequency cannot be propagated.

13. L. Spitzer, Jr., "Physics of Fully Ionized Gases," Interservice Publishers, Inc.

These evanescent noise waves will decay, in the region of the potential minimum at the cathode, so that noise excitation at the input section of the helix is considerably reduced.

In addition, the average charge density,  $\rho$ , is related to the average velocity and current density by the equation of continuity.

$$\rho = \frac{J}{V} \quad (10)$$

This suggests that the maximum charge density takes place at the maximum depressed potential region. If the space-charge density increases, the plasma frequency is raised and the noise band, which cannot be propagated beyond the potential minimum, is extended to higher frequency values.

Two curves of theoretically optimum noise figures versus frequency, based on the dispersion equation (9) given above, are shown in Fig. 7 for two levels of current density. The area to the left of each curve describes the cut-off region that is related to a fixed level of beam current. These curves indicate that, for a fixed beam current density, tubes designed to perform at a lower microwave frequency can achieve lower noise figures than those designed to operate at a higher frequency.

An interesting comparison of the plasma frequency cutoff curves with the results achieved by many experimenters is shown in Fig. 7. Special electron guns, designed to take advantage of this effect, are discussed in Section VI of this report.

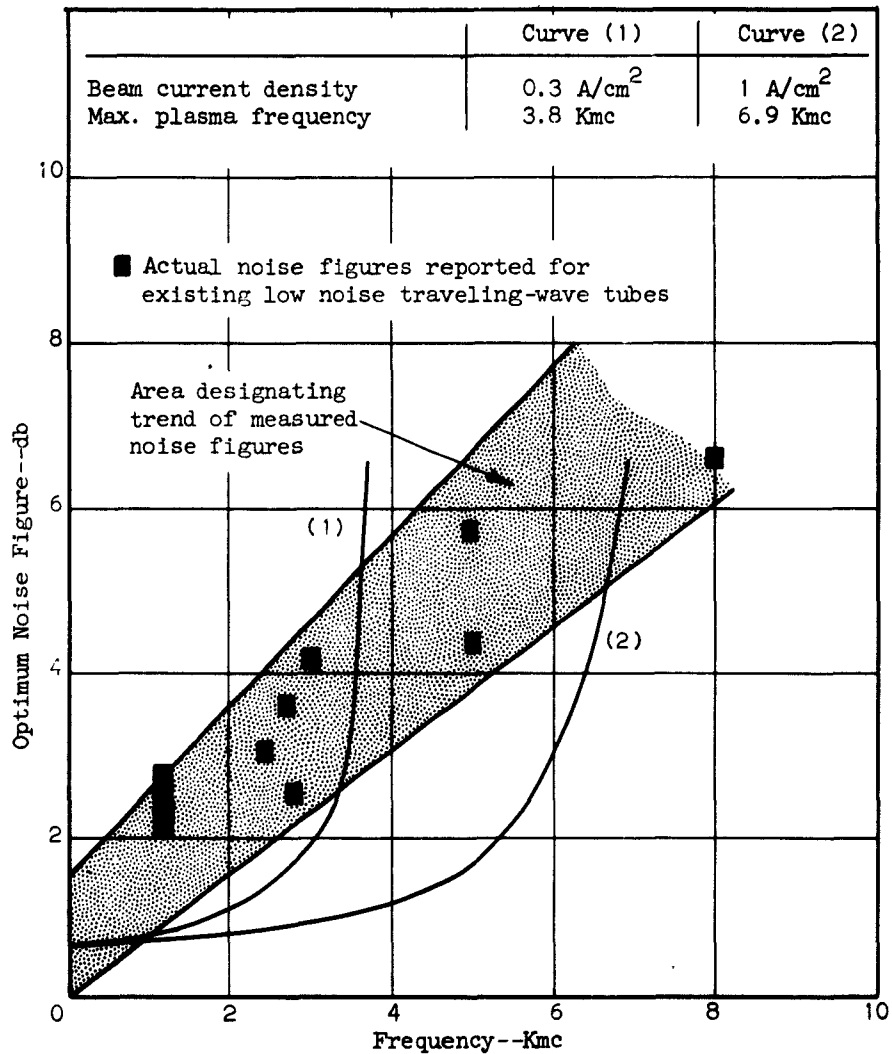


Fig. 7 - Theoretical optimum noise figure vs. frequency for various current densities.

#### IV. THE TRANSFORMER OR IMPEDANCE-MATCHING SECTION

To insure very low noise tube performance, the impedance-matching section of the electron gun, which interlinks the source of electron emission with the input to the rf slow-wave structure, must be carefully designed. A transmission line analogy of the exponential electron gun, introduced by Bloom and Peter,<sup>14</sup> of the RCA Princeton Laboratories, has led to the design of an outstanding impedance transformer. In this approach, the low impedance of the beam at the cathode is smoothly transformed into the high impedance required at the helix input section, consistent with requirements for minimizing the noise figure of the fundamental and higher order noise modes. Although other means of impedance transformation have been proposed and utilized for the low-noise traveling-wave tube, the exponential transformer is a preferred method because of its flexible operating characteristics. The exponential transformer, unlike the potential jump gun, for example, does not introduce abrupt potential changes and an associated lens effect which have been shown to increase noise under certain conditions.<sup>15</sup>

Although the exponential transformer method of impedance matching is preferred for the proposed interim tube, a thorough investigation will also be made of Einzel-lens-type impedance transformers. The Einzel-lens method, which has been used effectively in several RCA medium-noise tube designs, uses the focusing action of a weak lens to relocate the cathode "image," or more correctly the potential minimum in front of the cathode, so that it occurs at the input region of the slow-wave structure. This

14. S. Bloom, R.W. Peter, "A Minimum Noise Figure for the Traveling-Wave Tube," RCA Review, Vol. 15, p. 252, June 1957.

15. R.C. Knechtli, "Effect of Electron Lenses on Beam Noise," Trans. IRE, PGED p. 84, April 1958.

method of transformation is quite effective, in that some measure of noise reduction is achieved in the transformation scheme itself, which is not possible with the normal exponential transformer. Apparently, the aberration in the Einzel-lens system effectively reduces the axial velocity spread at the electron cathode "image" below that at the cathode "object," which is at the potential minimum. Recent investigations have shown this scheme is both theoretically sound and physically practical, and it may be possible to exploit the Einzel-lens transformation effect in the proposed tube design.

#### V. RF TRANSDUCER SECTION AND INTERACTION REGION

In addition to an optimum low-noise electron gun design, very low noise tube performance also requires an optimum design of the interaction elements (helix and beam). Primarily, the helix should be designed to obtain the best possible space charge modes through minimizing the space-charge factor,  $QC$ , while maintaining the gain factor,  $C$ , reasonably high.

The gain per unit length should be made as high as feasible, by increasing the helix impedance and the beam-helix coupling to minimize the effect of helix losses. The beam diameter is chosen to provide a satisfactory compromise between beam-helix coupling and minimum intercepted current. The helix distributed loss,  $L$ , should be reduced by silver plating the helix, by using low-loss helix supports, and by choosing a wire diameter-to-helix pitch ratio of 0.3 to 0.6.

In general, the design entails a relatively high TPI, small diameter, silver-plated helix supported in precision glass tubing by three ceramic rods clamped around the helix. This general structure, which is used in the RCA Type 6861 design, is not only a very low-loss structure, but is also very rugged and capable of an excellent gun-helix alignment. This alignment is an important item in very low noise tube designs because of the relatively high beam diameter-to-helix diameter ratios used.

Although emphasis will be placed on a three-rod-supported-helix, the "thermometer type" fluted glass-supported-helix structure will also be investigated. This type structure would enable a significant reduction in the tube capsule diameter which, in turn, would permit the design of a smaller, more efficient focusing solenoid, and would enhance the possibility of using periodic-permanent-magnet focusing. Some preliminary tests, made on low-noise thermometer-type tubes using helical couplers have shown these tubes to have a noise performance comparable with that of the three-rod structures. An increase in noise figure of approximately 0.25 db was observed in the thermometer-type tubes, which was probably due to increased coupler and tube helix losses.

Precision helix-winding techniques are now being used to minimize the possibilities of rf reflections from the helix. Highly efficient, lumped-loss type internal attenuators (lossy material sprayed on support rods) can provide the necessary rf isolation of the input and output signals for the three-rod-supported helix structure. The fluted-glass structure can make use of efficient coupled-helix type attenuators.

The coupling system used in the RCA Type 6861 design uses a modified coaxial cavity, which is voltage-coupled to an antenna at the end of the tube helix. Such couplers are capable of low-loss coupling over reasonable bandwidths. For example, in the type 6861 design, coupling over the range of 2.7 kmc to 3.5 kmc, with a cold VSWR of less than 1.5 and a coupling loss in the order of 0.3 to 0.4 db, is readily achieved. It is possible to achieve, at very low coupler losses, a cold VSWR of less than 1.2 over narrow frequency bands with these couplers. Thus, for the proposed interim tube design, use of these coaxial type couplers is preferable.

In summary, some of the problems and techniques that must be coped with in the development of a very low-noise traveling-wave tube have been considered. The state of the art in this field is undergoing constant changes as more is learned about the noise behavior of electron beams, both from the purely theoretical analyses and from empirical data based on experimental results. The main support for any theory must, in the long run, be supplied by consistently reproducible experimental evidence. It will be the purpose of the next section of this report to present some experimental data, past and recent, supporting some of the theoretical considerations discussed in this section.



### SECTION III

#### EMPIRICAL RESULTS

##### I. PRELIMINARY TESTS AND EVALUATIONS

Although the experimental investigations of low-noise traveling-wave tubes, which have been conducted by the RCA Microwave Design and Development Group, cover a wide range of frequencies and power levels, most of this investigative work revolved around the low-noise electron gun developed for the RCA Type 6861 tube. For this reason, this section of the report gives a brief review of the development of the basic electron gun for the 6861 tube. This electron gun is now used as a model the world over.

##### A. Development of the RCA Low-Noise Electron Gun

The history of low-noise traveling-wave tube work at RCA goes back to the year 1949, when the RCA Princeton Laboratories announced a heretofore unheard of noise figure of 16 db in a traveling-wave tube operated at S-band frequencies. This achievement was the basis for the development, in 1952 of a traveling-wave tube which used a multigrid electron gun and a modified exponential transformation to transform the effective beam impedance at the potential minimum to the impedance desired at the helix input.<sup>16</sup>

The exponential transformation minimized the amount of noise increase in the impedance-transformation region above that existing at the potential minimum and in addition, it permitted adjustment of both the noise-current standing-wave ratio and the position of the noise minimum in the helix-input region. These adjustments were made by varying electrode potentials over a

---

16. A.L. Eichenbaum, R.W. Peter, "The Exponential Gun - A Low-Noise Gun for Traveling-Wave Tube Amplifiers," RCA Review, Vol. XX, No. 1, March 1959.

range that did not appreciably affect beam currents or tube gain. However, because the helix losses were relatively high and no noise-reduction mechanisms (except that of space-charge smoothing of current fluctuations at the potential minimum) were used, the best noise figure that could be obtained in the multigrid tube was approximately 8 to 9 db at S-band frequencies.

From 1953 to 1955, under a program sponsored by the Lincoln Laboratories of MIT, the RCA Microwave Design and Development Group at Harrison, N. J., worked to improve the tube developed by the RCA Princeton Laboratories. The aims of this program were to develop a traveling-wave tube readily adaptable to production manufacturing techniques and capable of consistently reproducible low-noise performance.<sup>17</sup> The development program was very successful, and the final tube design that resulted is now known as the RCA Type 6861. The major achievements of the program were:

1. The establishment of techniques for fabricating and processing oxide-coated cathodes for low-noise performance.
2. The design of a very low-loss, high-impedance helix structure.
3. The redesign of the Princeton low-noise electron gun into a configuration which empirically gave the lowest tube noise performance.

Of the above achievements, the redesign of the low-noise electron gun was the most important, for this enabled the achievement of tube noise figures (see Fig. 8) below what was then considered the theoretical limit, as given by the single-velocity approximation theory for traveling-wave devices.

---

17. "Low-Noise, S-band Traveling-Wave Tube," Final Report, Subcontract No. 31, under AF19(122)-458, Lincoln Labs., M.I.T.

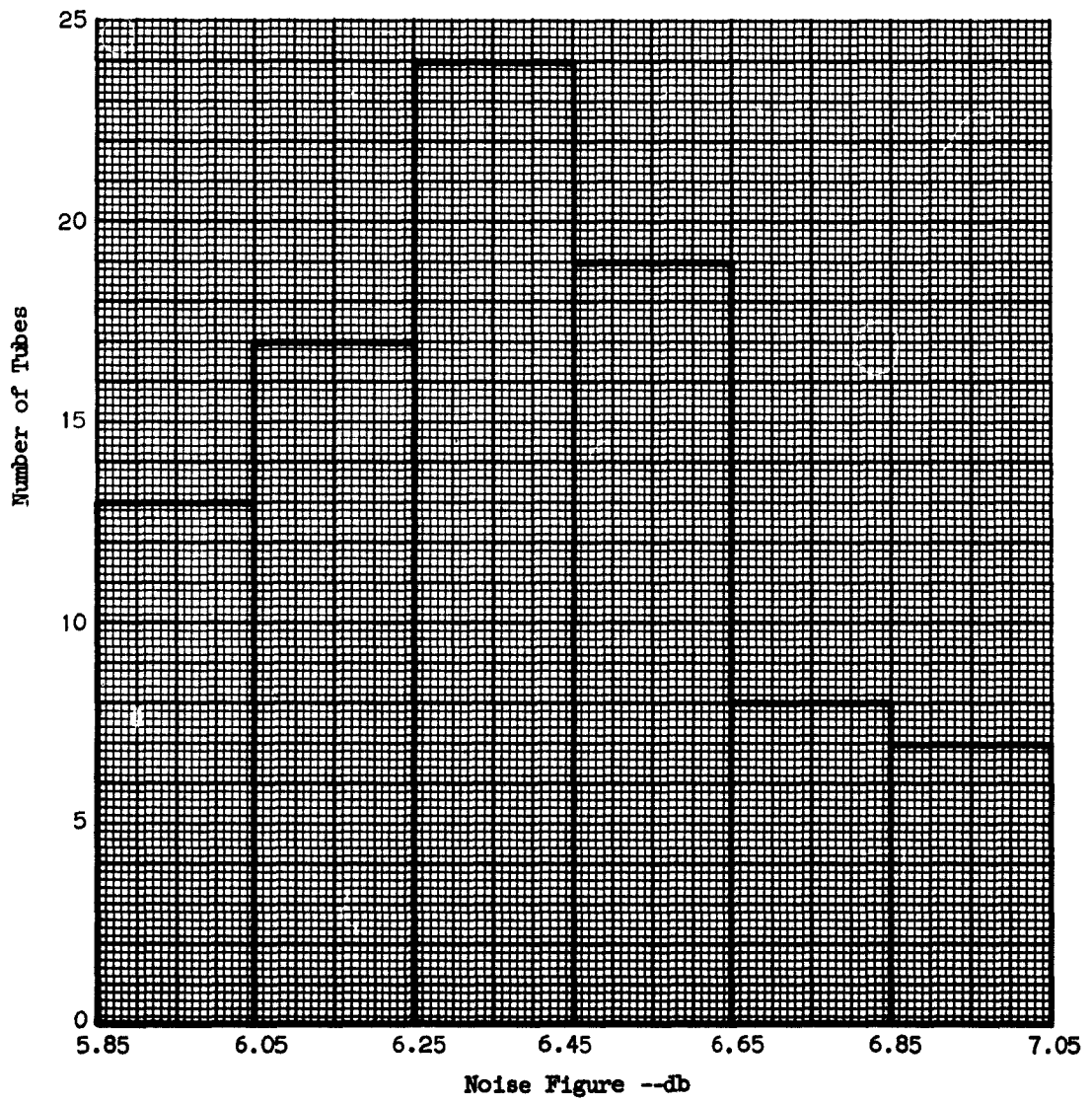


Fig. 8 — RCA Type 6861. Noise figure distribution in 88 tubes.

### B. The Basic Type 6861 Low-Noise Gun Design

The noise reduction techniques employed in the cathode-anode region, the impedance-transformation region, and the rf circuit region of the type 6861 tube are discussed below.

1. Cathode-Anode Region - Although the very low helix losses of the 6861 design contribute greatly to low-noise performance of this tube, the major factor, in the achievement of the low-noise performance, is the novel divergent-beam-launching technique used in the 6861 design. However, optimum beam-launching conditions were determined empirically, and some attempts were made to correlate the divergent launching of the beam with the improved noise performance during the development of the 6861 tube. In light of the knowledge gained since 1956, subsequent to the development of the 6861 tube, the development of the divergent-beam-launching technique was a very significant achievement.

The basic cross-section and some typical operating potentials of the electron gun in the type 6861 design are shown in Fig. 9 (a). The region between grids No. 1 and No. 2 can be considered the beam-launching or cathode-anode region, and the region between grids No. 2 and No. 4 can be considered as the main section of the exponential impedance transformer. A typical beam-edge potential profile for this tube is shown in Fig. 9 (b). The optimum tube noise figure is obtained primarily through adjustment of the impedance transformer by varying the potentials on grids No. 3 and No. 4.

The gun geometry was adjusted so that optimum noise performance was obtained with grid No. 1, the beam-forming element, operating at zero bias and the magnetic field at about 525 gauss. The position of the cathode in relationship to the shaped-beam former, grid No. 1, partly determines the

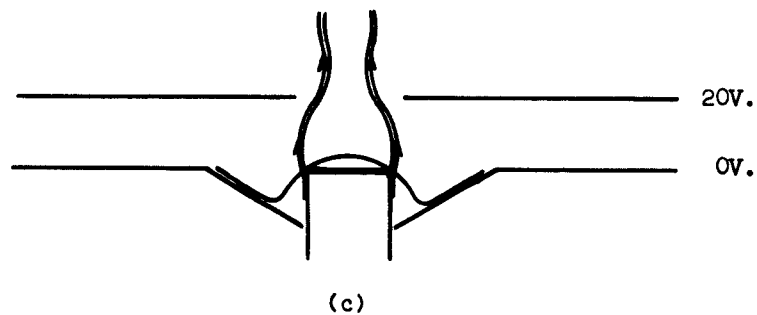
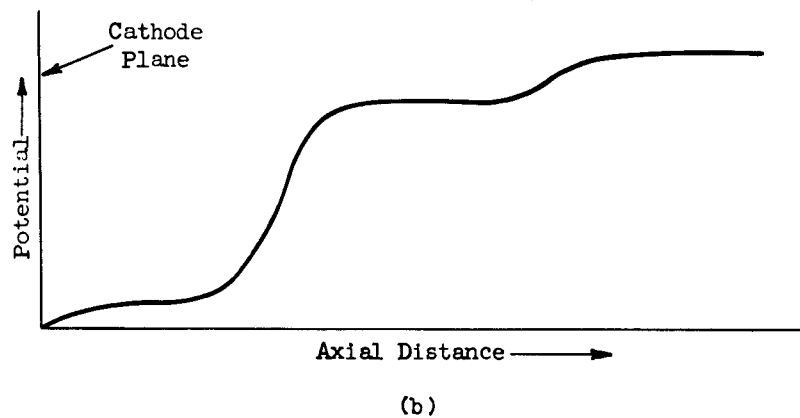
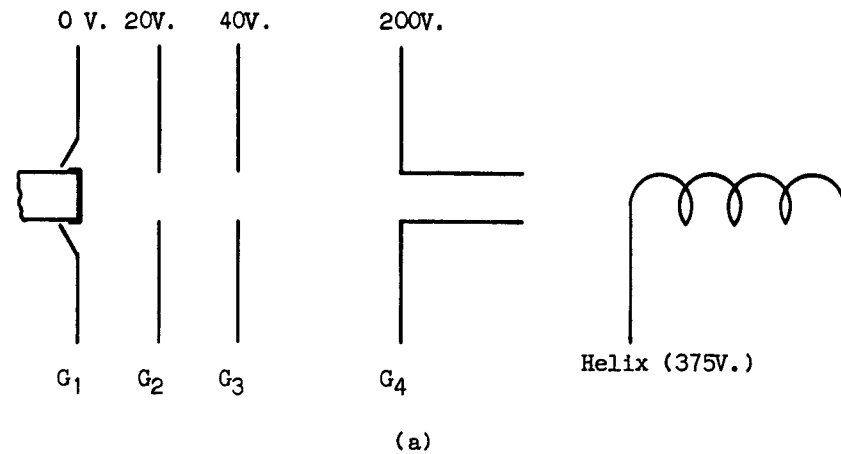


**Fig. 9 — Basic features of the RCA Type 6861 low-noise electron gun. (a) Cross section of electron gun. (b) Beam-edge potential profile. (c) Beam launching characteristics.**

configuration of the two-dimensional electric field at the cathode. This configuration is such that the potential profiles are distorted about the planar cathode in such a way that most of the cathode emission is limited to a region of less than a 0.005-inch width at the cathode periphery. (See Fig. 9 (c).)

a. The Hollow Electron Beam - The beam of the 6861 tube is of the dirty-hollow-beam type in that most of the emitted current is concentrated in the very thin shell at the cathode periphery, and the current density diminishes rapidly in the direction of the cathode axis. Therefore, the noise performance of the 6861 tube is very much dependent upon the nature of the cathode coating at this periphery. In fact, most noise-figure increases in these tubes can be traced to cathode damage (partial sintering of the coating, loss of coating in spots, and excessively granular coating) in this region.

Special tubes, constructed both prior to and during the early part of this program, in which the normal planar cathode was replaced by thin annular cathodes, have shown no appreciable difference in the electrical performance of the tube, even though in one instance the annular thickness was reduced to approximately 0.004 inch. These results confirm the hollow nature of the electron beam in the 6861 design.

Figure 10 shows the noise-figure variations as a function of tube parameters for a typical 6861 tube which has a well-processed low-noise cathode. Empirical results show that, under standard 6861 test conditions (tube parameters as shown in Fig. 10), the hollow electron beam expands to about 1.2 times the normal cathode size in the cathode-anode region. The

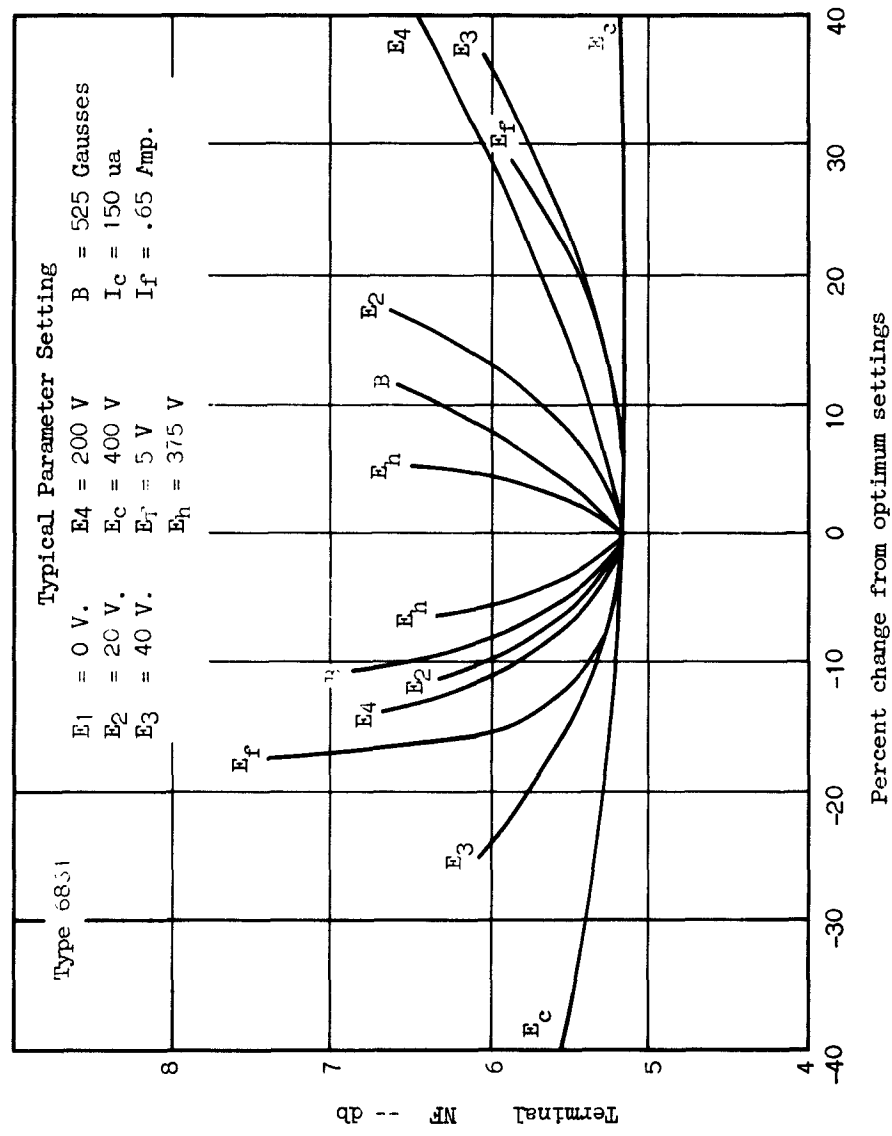


Fig. 10 -- RCA Type 6861. Noise-figure variation with tube parameter adjustment.

significance of this expansion, both from the viewpoint of potential gradient and crossed-field conditions, was discussed in Section II of this report.

As shown in Fig. 11 and as expected from the crossed-field theory of noise reduction, the noise figure of the 6861 tube is a function of the magnetic field for a particular beam-launching condition. This relationship is even more apparent in Fig. 12, where the noise figure versus magnetic field strength is plotted for a type 6861 tube operated under a fixed beam-launching condition. For the particular launching condition chosen, the noise figure was minimized at magnetic field strengths of approximately 600 and 1100 gauss. This behavior is expected if noise reduction, due to crossed-field effects, occurs when the hollow beam precesses to the reference plane in an integral number of revolutions. As shown in Fig. 12, when the beam-launching angle ( $\phi$ ) increases, the periodic effects become even more pronounced. Some of this periodicity is due to reflected electrons from the collector region, but these effects can be eliminated through use of very high collector potentials, or specially designed collectors.

b. Optimum Electron-Gun Operation - Optimum electron-gun operation, in regard to low-noise figure achievement, is obtained when the beam launching angle ( $\phi$ ), as given in Fig. 5 (b) has been properly adjusted. This adjustment is accomplished by varying the potentials on grids 1 and 2 to achieve maximum noise reduction at the transformation reference plane for the particular current density and magnetic field being used. Under fully optimum conditions, and primarily because of a reduction in the crossing of electron trajectories in the laminar-type beam flow, the noise figure is



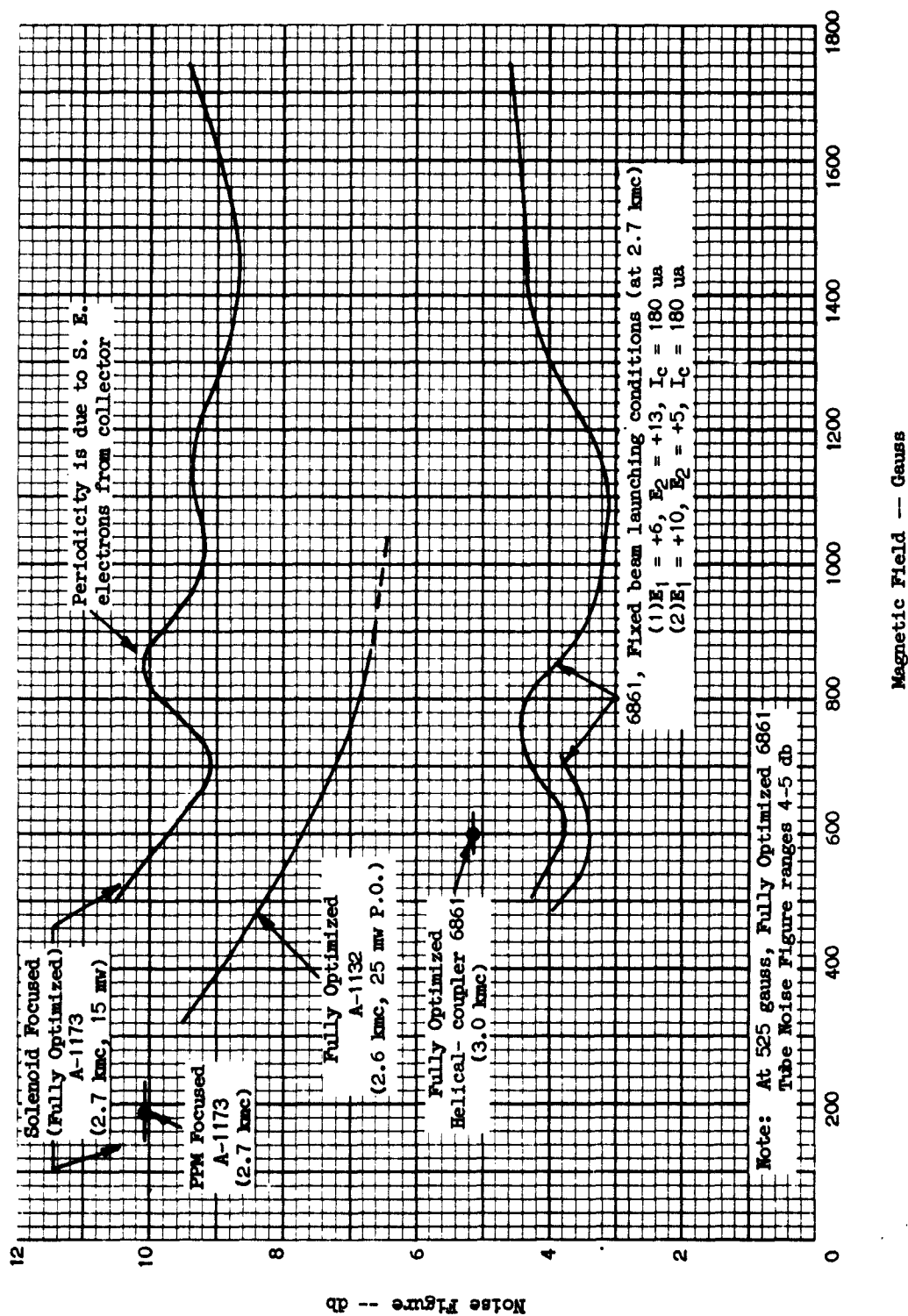


Fig. 11 -- Experimental tube-noise figure results with modified type 6861 and other tube designs.

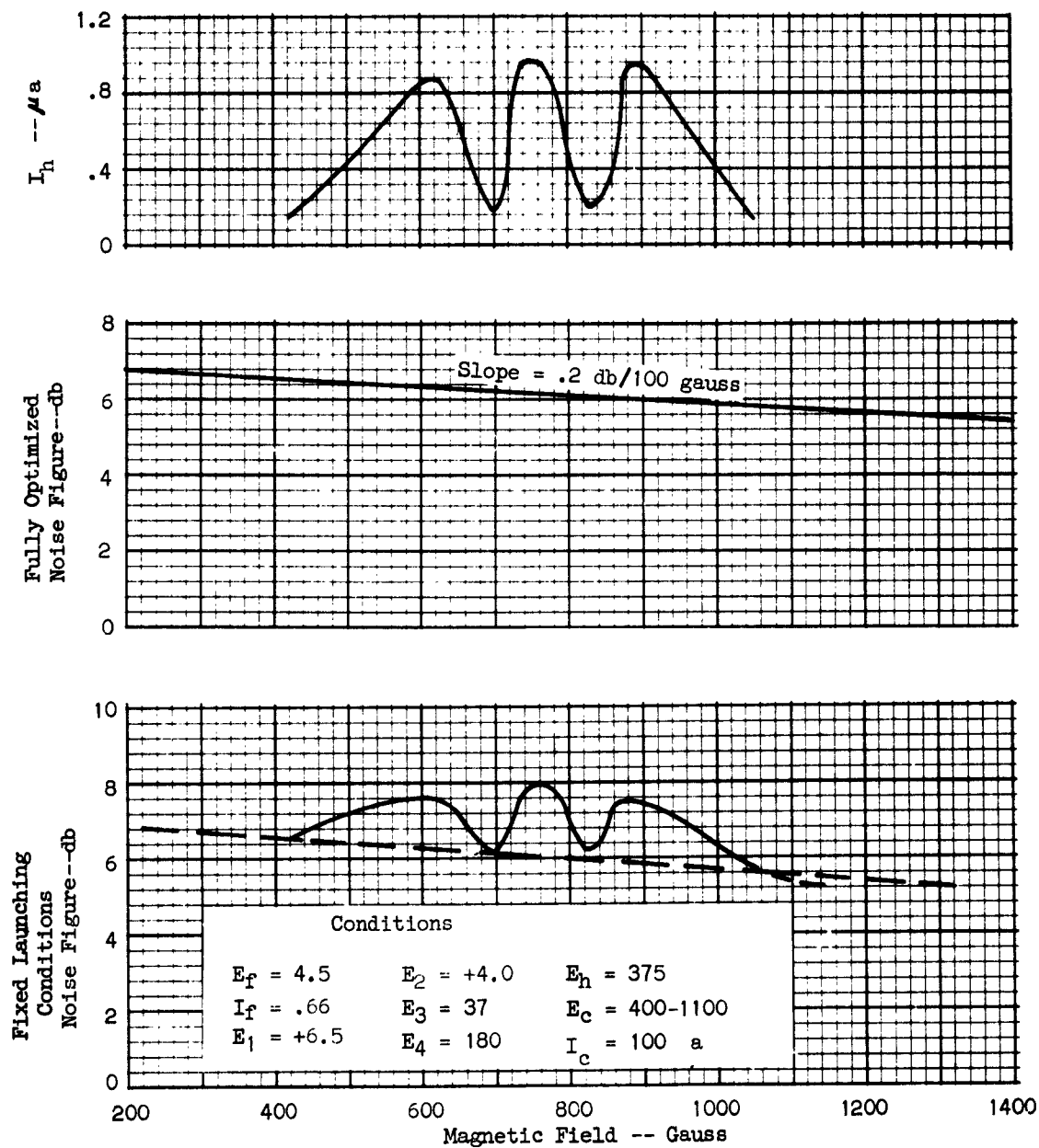


Fig. 12 — Cyclic behavior of noise figure vs. magnetic field for type 6861 in which launching angle ( $\phi$ ) is relatively large.

expected to improve monotonically with increases in the magnetic field. This behavior is shown for an RCA Type 6861 tube in Fig. 13. It is also applicable to higher-power tubes using the basic 6861-type electron gun, as shown in Fig. 11, where the noise figure versus magnetic field is plotted for tubes with 15-mw and 25-mw outputs.

The limiting point for noise reduction due to crossed-field effects in the beam-launching region is determined largely by the electrostatic controls over launching that are available in this region. For the standard 6861 electron gun geometry, this noise-reduction limit is reached when the magnetic field strength is approximately 1000 gauss. (See Fig. 13.) A more graphic illustration of this electron-optical limitation is shown by the approximate plots of beam-edge potential profiles, shown in Fig. 14. To more clearly define the beam-launching characteristics in the cathode-anode region, additional and more closely spaced potential-profile-determining elements are required. Also, as shown in Fig. 14, for stronger magnetic fields, the two-dimensional characteristic of the electric field increases, and this results in a reduction in the axial velocity of the electron beam -- a condition that is also necessary for increased correlation effects between current and voltage fluctuations in the beam in the cathode-anode region.

2. Impedance-Transformation Region - The normal 6861 design uses the modified exponential impedance transformation, described in Section II of this report, to minimize noise increases and to electrically locate the noise minimum at the optimum point in relation to the circuit input plane. Figure 14 also shows the typical beam-edge potential profile that produces such a transformation characteristic.

As pointed out in the theoretical noise studies of Section II, it is possible to obtain an additional noise reduction, in the transformation

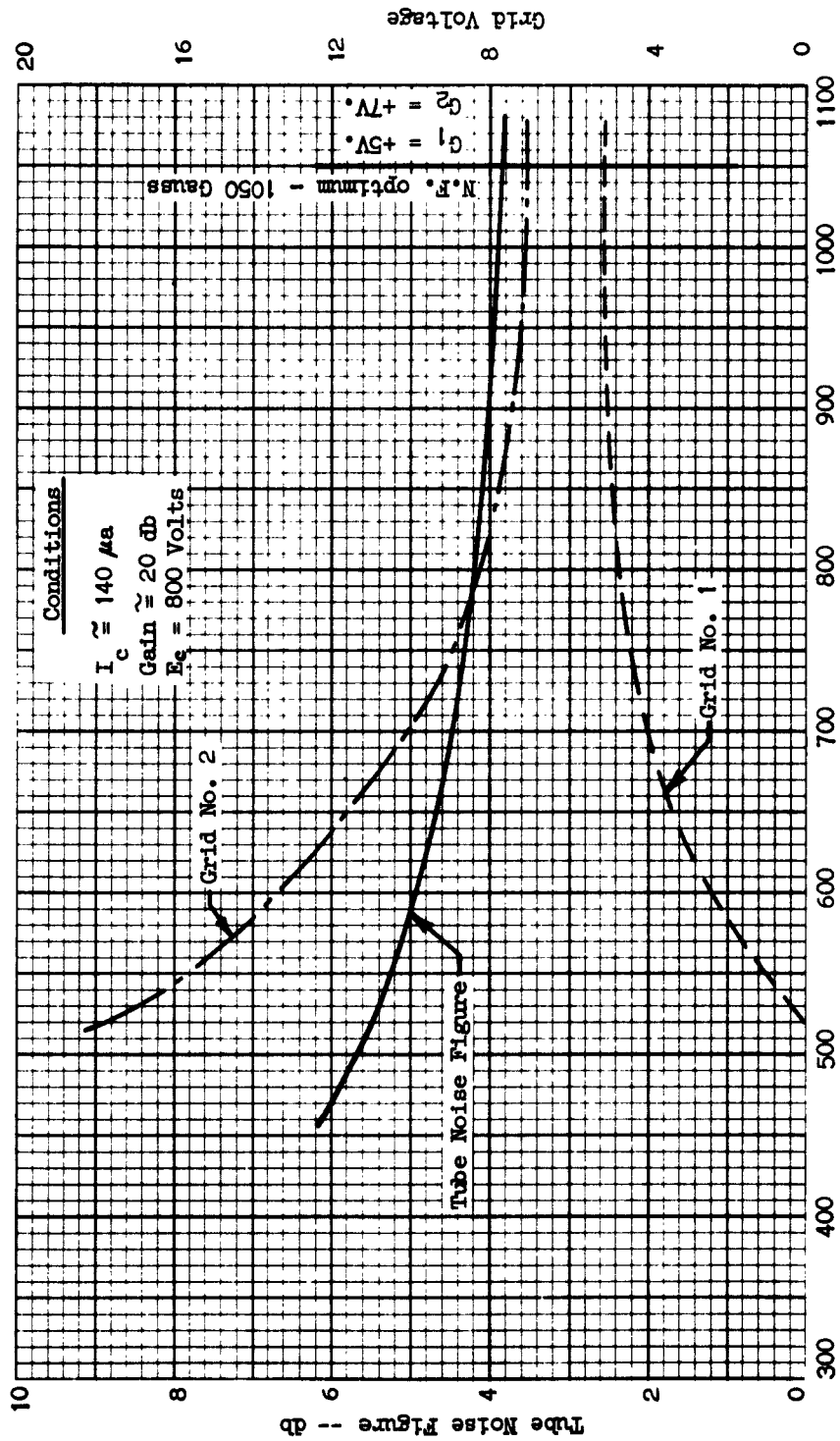


Fig. 13 - Beam launching characteristics of a single RCA Type 6861 tube (Ser. No. 179).

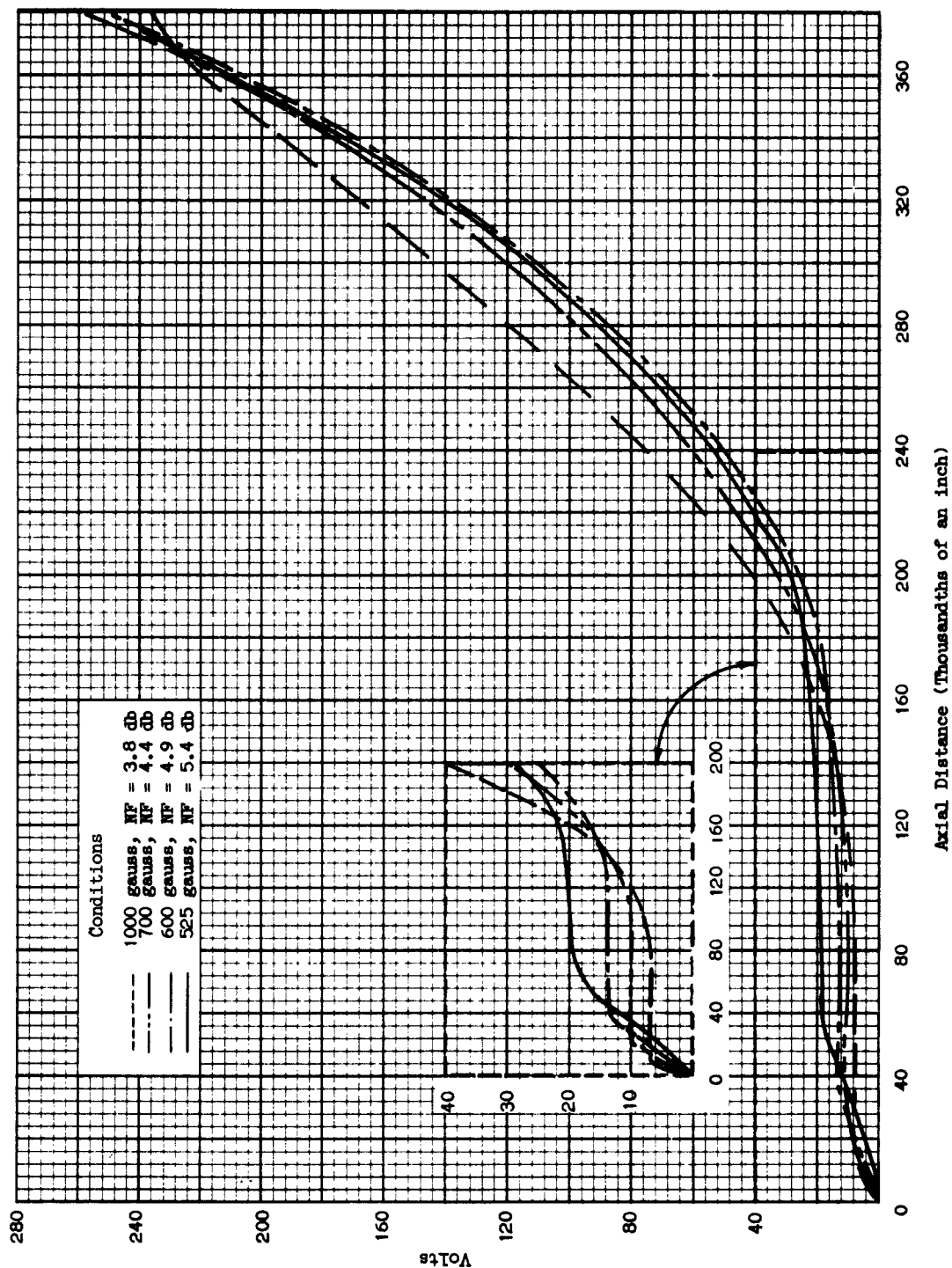


Fig. 14 - Beam edge potential profile of a single RCA Type 6861 tube (Ser. No. 179).

region, by a further reduction of the spread in electron velocity classes. However, when noise reduction is achieved in this manner, the velocity fluctuations are no longer invariant in the transformation region, because the energy relations in the beam are disturbed. As pointed out in Section II, the Einzel lens transformation effectively reduces the velocity spread in the beam in the interaction region compared to the spread at the virtual cathode, which is located in the gun region.

The Einzel lens transformation was first used in periodic-permanent-magnet-focused low-noise tubes in which crossed-field reduction in the cathode-anode region could not be used because of the very low magnetic fields required for the electron guns of these tubes.<sup>18</sup> The use of the Einzel lens transformation instead of the modified exponential-type transformation, which is usually employed, reduced beam noise at least 50 percent.

The Einzel-lens mechanism was applied to the basic 6861 electron gun by adding extra gun elements in the transformation region. Some experimental results of Einzel lens effects are shown in Fig. 15. Two types of Einzel lenses were used in this particular test; one with its center electrode positive, the other with its center electrode negative. The best results were obtained with the center electrode negative, as shown by Curve A, Fig. 15. The ultimate noise performance was degraded because of excess noise generated by a defective cathode, but the effect of the mechanism is quite apparent in the curves of Fig. 15. Similar effects for another multigrid 6861 design are shown in Fig. 16. The ultimate noise performance of this design was also degraded due to excess gas levels

18. G. Hodowanec, W. Poelstra, and J.N. Nelson, "A Family of Medium-Noise Periodic-Permanent-Magnet-Focused Traveling-Wave Tubes," Presented at IRE Electron Devices Meeting, Washington, D.C., October 1959.

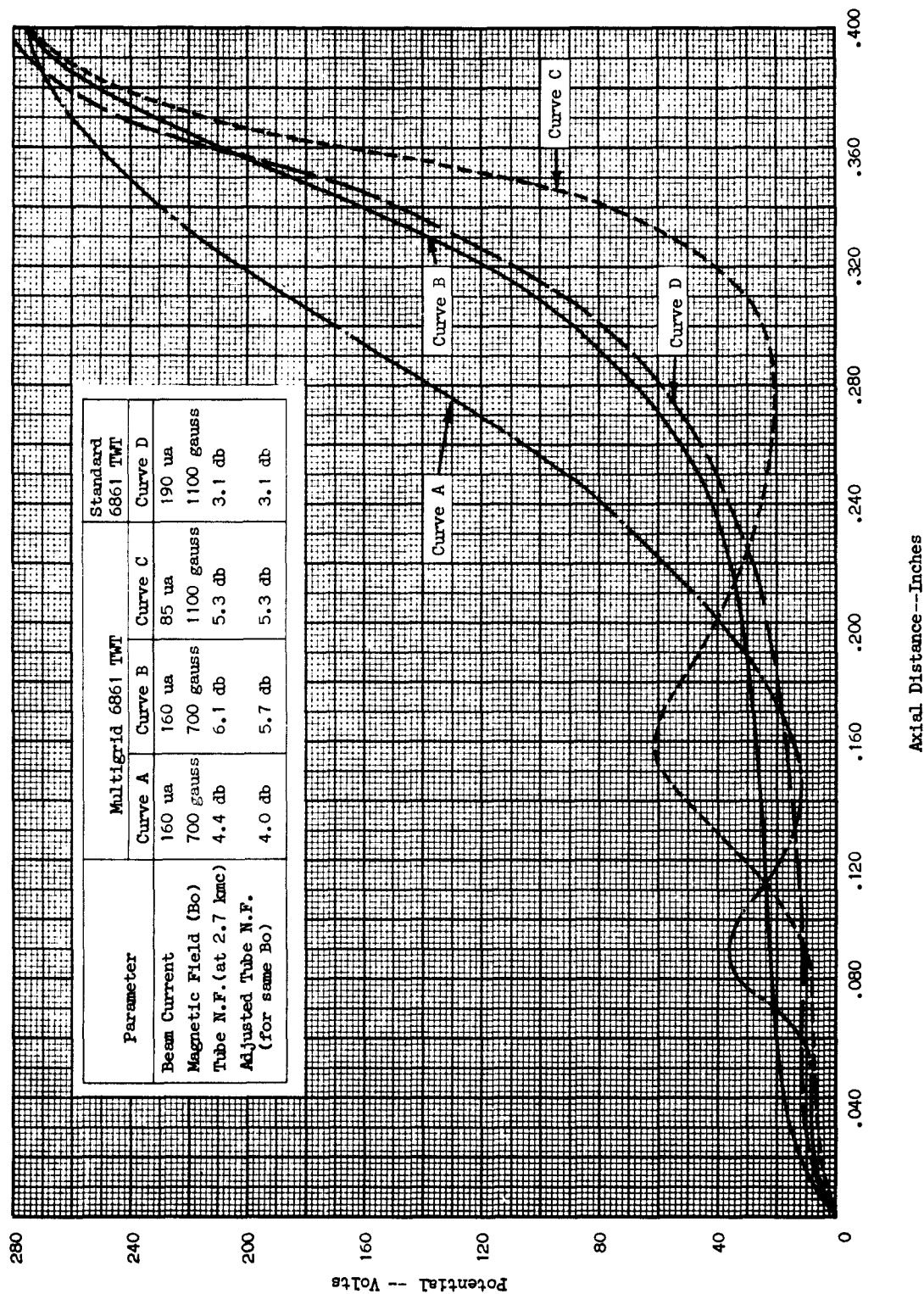


Fig. 15 — Effects of Einzel-Lens type impedance transformation on tube noise figure in the basic type 6861 design.

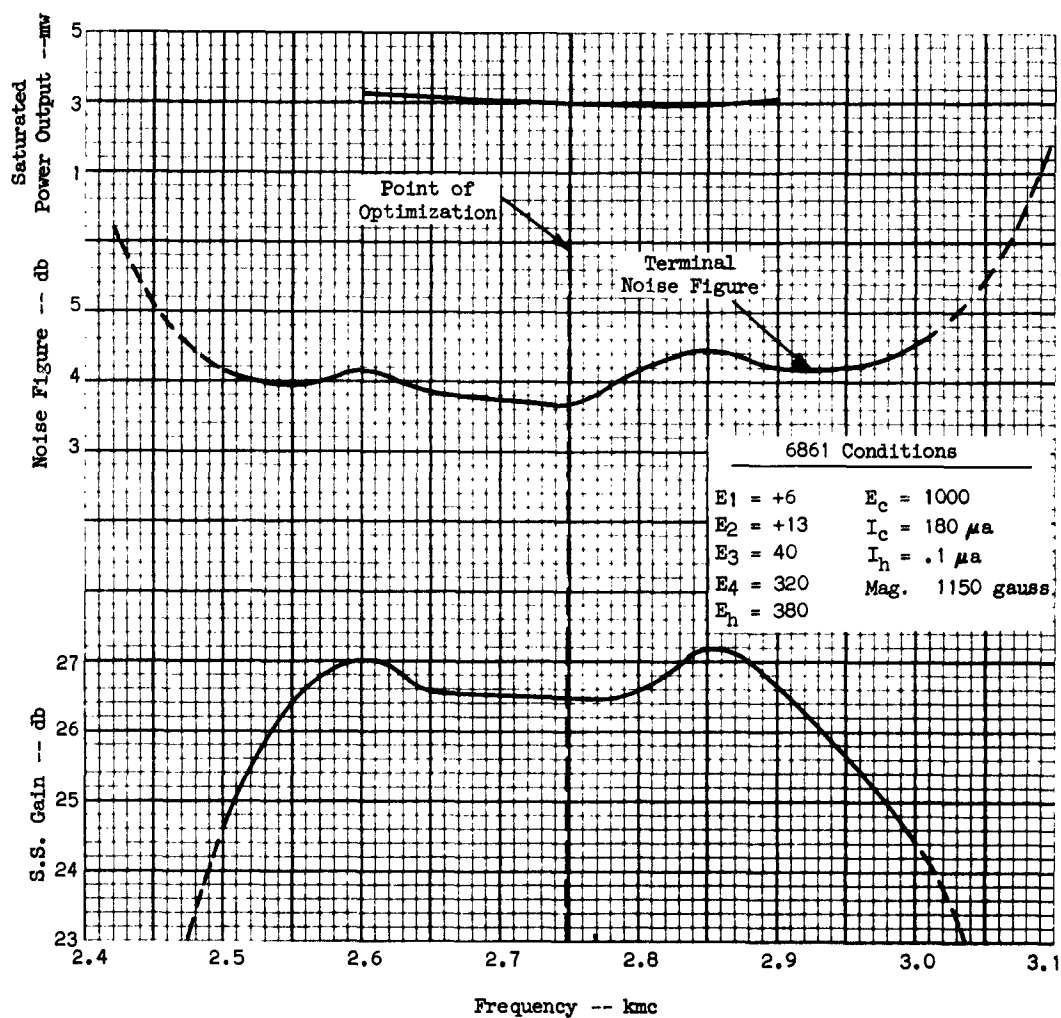


Fig. 16 — Approximate beam edge potential profile for modified multigrid 6861 tube design.



in the particular tube tested. Investigations of this type will continue during this development program.

3. The RF Circuit - The primary requirements of the rf circuit—couplers and helix—were discussed, to some extent in the theoretical section. For the type 6861 design operating under standard conditions, the circuit losses are quite low; thus, the tube noise is primarily limited to that of the beam noise, as determined by the electron gun conditions. Under fully optimum conditions, the beam noise is reduced to the point where, again, circuit losses, especially coupler losses, become an appreciable factor in determining the terminal tube noise figure.

Figure 17 shows the rf performance of a standard design type 6861 operated under optimum conditions. Here, optimum tube performance is limited to the frequency range 2.5 to 3.0 kmc primarily because this is the only region of fair coupler match for this particular tube in this particular capsule. Coupler match is, therefore, a limiting factor in the rf performance of the 6861 design, and work is planned, during this program, to improve the design, both from the viewpoint of coupling bandwidth and coupling losses.

#### C. Summary of Preliminary Experimental Results

In summary, the experimental results described in this section have applied generally to the 6861 type of low-noise tube design. The fundamentals of the low-noise electron gun design, as expressed by the basic 6861 design, also apply to other low-noise designs in which circuit losses are much higher than those found in the basic type 6861 helix-coupler design. In such designs, the noise-performance degradations are a direct function of the circuit losses, but the basic beam noise remains a function of the

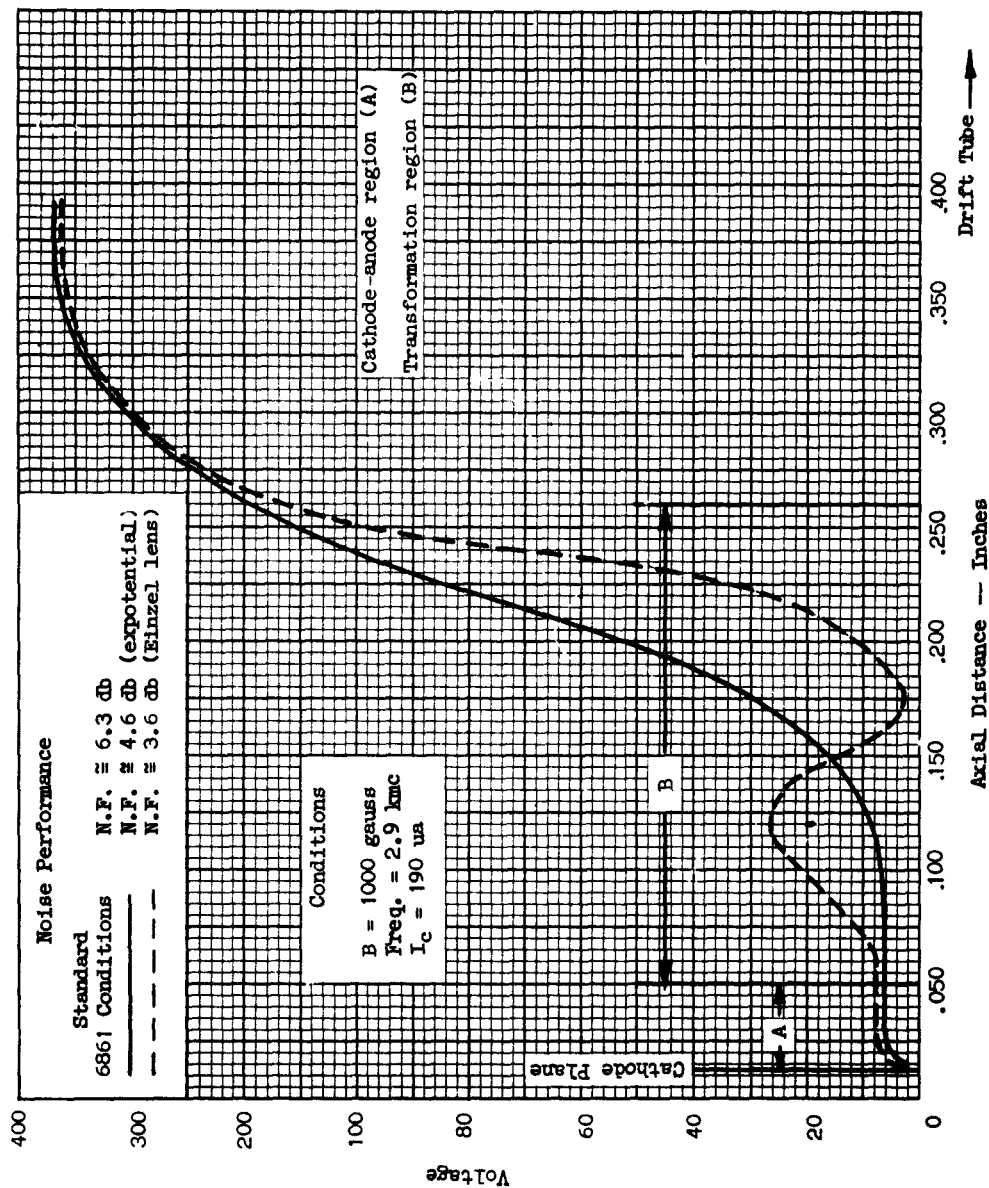


Fig. 17 - RCA Type 6861. Gain, power output, and noise figure under fully optimum conditions.

electron gun design. This is an important conclusion, since it means that the low-noise performance of a relatively good low-noise traveling-wave tube design (such as the type 6861) can be improved only by further reduction in the basic noisiness of the electron stream. How this may be accomplished in a practical design is considered in paragraph II of this section.

## II. NEW LOW-NOISE ELECTRON-GUN DESIGNS

Some of the premises of low-noise electron gun design were given in the theoretical noise treatise of Section II. Experimental verifications for some of these premises were shown in the analysis, given in paragraph I of this section, of the data obtained from tests on the type 6861 design or on designs using the basic 6861 type low-noise electron gun. The lower noise-figure limit of the basic 6861 design, as it is now used, was shown to be in the order of 3 db. Further noise reduction in this type design requires:

1. Improved beam-launching characteristics for:
  - a. An improved crossed-field noise-reduction effect.
  - b. A reduced thermal velocity spread at the cathode.
2. Noise reduction in the transformation process.
3. Low-velocity launching to extend the region (see section II, paragraph I-A) so that correlation effects between current and voltage fluctuations in the electron stream will be increased.

### A. Modified 6861 Electron Gun Design

A new electron-gun design which permits the evaluation of a number of noise reduction techniques is shown in Fig. 18. This design, hereinafter referred to as design A, consists of a multigrid electron gun with a beveled cathode periphery. The cathode periphery -- the region of electron emission

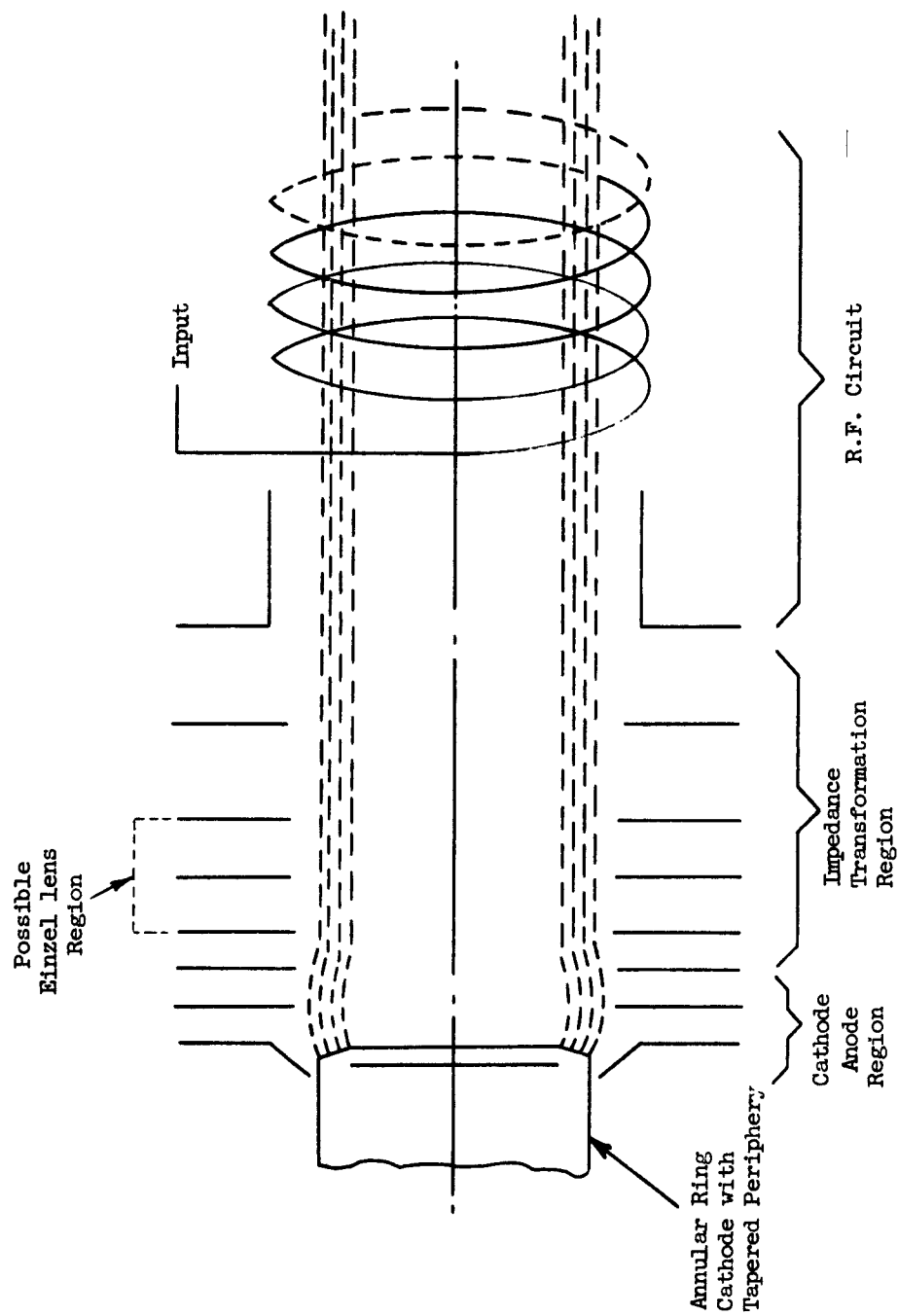


Fig. 18 -- Proposed structure for ultra-low-noise electron gun -- Design A.

in this design -- is beveled in the direction of emission to emphasize electron emission normal to the plane of the beveled periphery under the divergent launching conditions usually experienced in this design. To more clearly define beam-launching characteristics, under conditions of high magnetic and very low electric fields, the cathode-anode region is made a multigrid region. The transformation region is also made a multigrid region to enable utilization of the noise-reduction characteristics of the Einzel lens.

Basically, Design A will be used in instances of beam formation where the normal potential minimum, due to space charge effects, exist just in front of the cathode surface. The maximum current density in such a beam is limited by the electron-optical requirements, in this region, for the other noise-reduction considerations.

#### B. Created-Space-Charge Electron Gun Design

Figure 19 shows an electron gun design, design B, in which a second space-charge potential minimum exists. This potential minimum is created by means of electron optics (i.e., an Einzel lens) and is used to form a very dense space-charge region, which is independent of the cathode-anode conditions, and thus, is not limited by conditions at the cathode. Design B will be used primarily to evaluate the noise-shielding effects of a very dense space charge.

#### C. Electron Gun Evaluation Plans

During this program, emphasis will be placed upon Design A, since initial tests have indicated that this design is probably capable of additional noise-reduction, which cannot be fully exploited in the standard type 6861 design. A series of evaluation tests for designs of the general type, shown in Fig. 18,

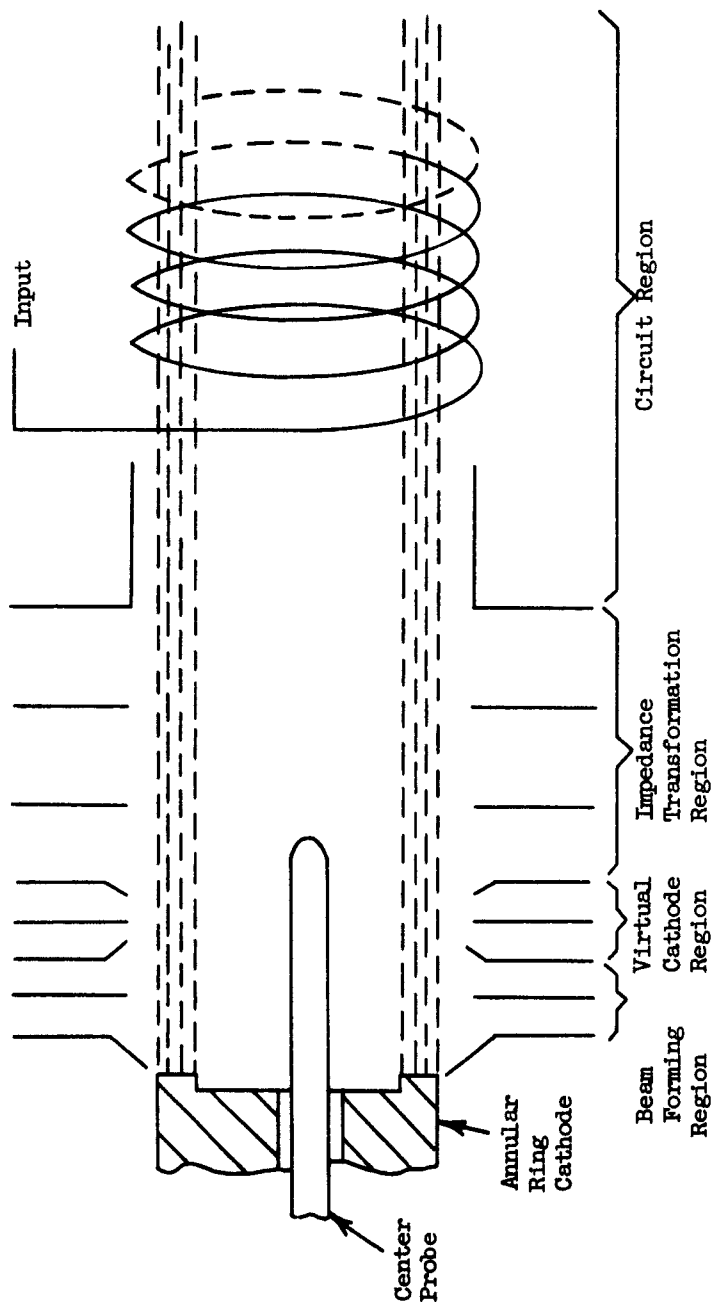


Fig. 19 — Proposed structure for ultra-low-noise electron gun — Design B.

were begun during this first phase of the development program. Cathode shapes and aperture spacing in the guns will also be modified in these tests.

### III. SOLENOID FOCUSING METHODS

The high order magnetic fields, required for constraining the very high density space-charge beam of the low-noise electron gun design, dictates the use, at present, of a solenoid as the source of this magnetic field. The use of solenoids not only enables generation of high-intensity magnetic fields, but also simplifies the problem of shaping and adjusting of the magnetic field to meet the requirements for optimum focusing and noise performance. The first proposed-tube-focusing package will use a two-section solenoid as shown in Fig. 20. The first test will be of tubes in a single-section, water-cooled solenoid.

The gun-field solenoid will supply the relatively high magnetic field (approximately 600 to 1200 gauss) required in the low-noise electron gun region. This field will extend from the tube cathode to a point beyond the helix input region. The field will be supplied (if possible) by an aluminum-foil type solenoid in order to minimize possible transverse magnetic field components. The absolute value of gun field can be made adjustable over a wide range of values by (1) the adjustment of solenoid current, and (2) the judicious use of flux guides (shims) to direct or enhance the magnetic circuit in the electron-gun region.

In the tube helix region, which is relatively smaller in outer diameter than the gun region, it may be possible to use a longer solenoid with a comparably smaller inside diameter to achieve the same order of magnetic field as that of the gun field.

The focusing scheme depicted in Fig. 20 permits three general modes of focusing. Mode I is basically that of a highly confined beam from the cathode to the anode. This mode has been used in most low-noise tube designs, and its features are well known.

Mode II is a modification of Mode I in that the magnetic field at the gun region is gradually reduced to the lower field that can be tolerated at the helix region. If the transition region is shaped properly, the beam can be transformed from a confined flow at the cathode radius to a confined flow at a slightly greater radius without the introduction of beam scalloping. The use of the Mode II scheme permits the design of a smaller solenoid for the helix region which consumes less power.

Mode III indicated that it may be possible to go from highly confined beam flow in the very low-noise gun helix-input region to quasi-Brillouin type beam flow in the remaining helix region. This type of operation may improve the stability of the hollow-type electron beam. In addition, the use of opposing solenoidal fields simplifies the achievement of high gun-field fluxes by the judicious use of flux guides (shims).

Most of the low-noise evaluation data given in this report were obtained with a uniform field solenoid using Mode I focusing. A special solenoid, with its windings modified to give the tapered-field characteristics of Mode II, was also constructed. The magnetic-field characteristics of this solenoid are shown in Fig. 21. RF evaluations of this focusing structure have not, as yet, been performed.



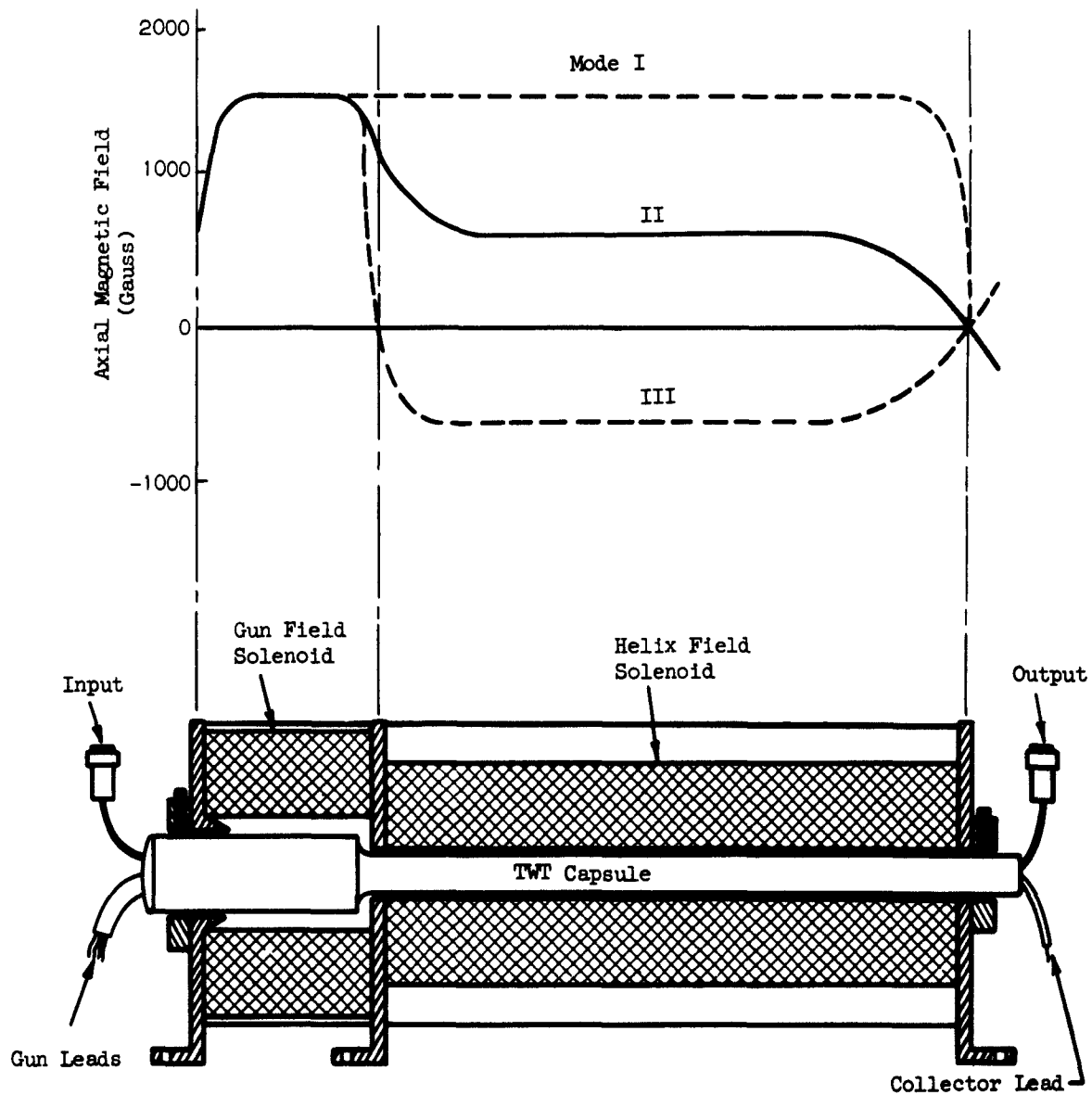


Fig. 20 — Proposed scheme for initial focusing package.

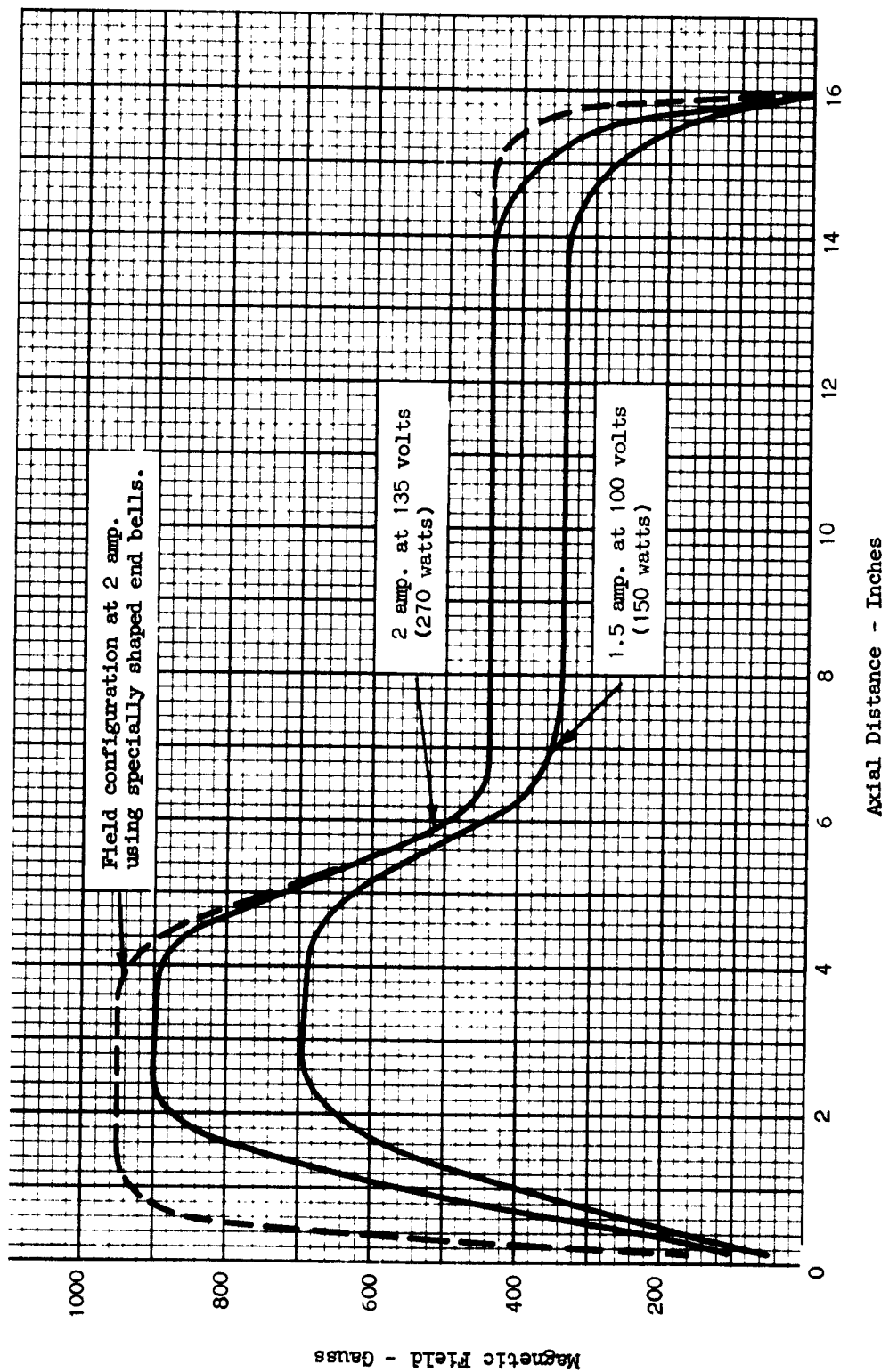


Fig. 21 — Tapered field solenoid characteristics.

## SECTION IV

### CONCLUSIONS

The theoretical studies, coupled with the experimental tests, which have been made during the beginning phase of this very low-noise traveling-wave tube development program, have indicated further noise-reduction possibilities in tube designs based on the 6861 as a prototype. This noise reduction can be achieved by:

1. Reducing beam kinetic voltage fluctuations.
2. Reducing beam current fluctuations.
3. Increasing the possibility of correlation effects between current and voltage fluctuations.

The theoretical studies and confirming experimental tests have indicated that all of these techniques could possibly be incorporated in a basic new electron gun design.

## SECTION V

### PROGRAM FOR THE NEXT INTERVAL

During the next quarter, the work will be devoted primarily to the evaluation of new electron gun designs and to the establishment of an interim design for the focusing solenoid. An interim electrical design of the very low-noise traveling-wave tube, using the type 6861 tube as its prototype, is planned for the end of the next quarterly period. Also, initial tests of the very low noise fluted-glass traveling-wave tube design are expected to be well underway.

The coaxial-cavity coupler studies, during the next quarter, are expected to result in designs which provide very low coupling losses over increased coupling bandwidths.

The very low tube noise figures being achieved during this program, require the early establishment of a new noise reference source, which has an accurately determined excess-noise output of a lower level than that now provided by the gas type noise source.

The basic low-noise theoretical studies will continue with the emphasis being placed upon the determination of correlation effects in the low-velocity electron stream, the effects of the Einzel lens on noise, and space charge noise shielding effects.

## APPENDIX A

### NOISE-FIGURE MEASUREMENTS

Noise figure is proportional to the amount of noise added by the traveling-wave tube to the original signal-noise ratio (assuming signal and noise receive the same tube gain). Therefore, the simplest method of measuring noise figure is to add an equal amount of noise at the traveling-wave tube input to double the traveling-wave tube output noise signal indicated on a display meter. The basic equipment to perform these functions is shown schematically in Fig. 22. In this method, the noise of the argon-bulb noise source (A) as reduced by the precision attenuator (B), is added to the traveling-wave tube noise to double the traveling-wave tube output as measured by receiver (D). A 3-db IF attenuator in Receiver (D) is then inserted between the tube and the indicator to provide the same reading as from the traveling-wave tube noise itself minus the 3-db attenuator. The NF is then the NF of the noise source minus the precision RF attenuator loss.

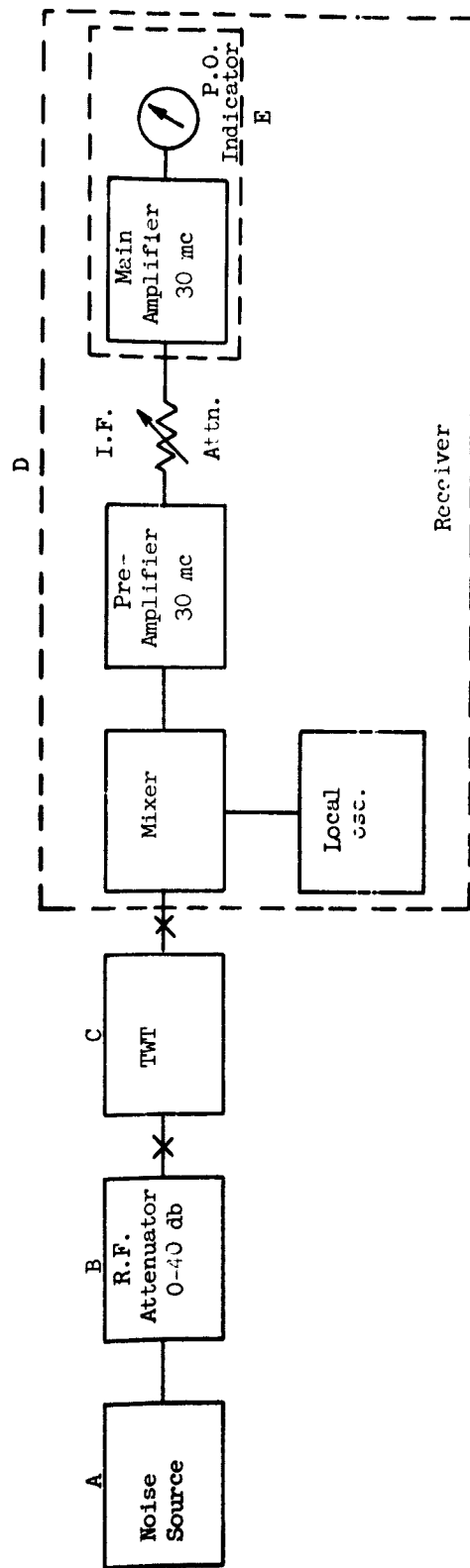
More precise NF measurements can be made by using the standard Y factor procedure utilizing argon noise sources. The set-up shown in Fig. 114 can be used except that normally the argon noise source feeds directly into the traveling-wave tube under test (Attenuator (B) is not used.) The tube under test is adjusted for minimum noise output as indicated by the power sensitive meter in the microwave receiver unit. (Note: Noise source off). A known amount of noise (from the calibrated argon-bulb noise source) is then added to the tube input. The meter reading increases Y db. This ratio is determined by inserting IF attenuation until the reading on the power meter is the same as has been determined with tube noise alone. The NF can be noted from

convenient charts plotting the inverse function of  $Y$  versus NF. This NF includes receiver noise. In most cases, this is negligible if the receiver gain is high, but can, if required, be subtracted out.

Rapid and direct noise figure measurements can be made using an automatic NF measuring unit such as the Hewlett-Packard Model 340A. This unit is inserted in the receiver section marked (E) in Fig. 22.

In the measurement of tube noise figures of less than 5-db, extra care must be used in determining the amount of added noise (i.e. temperature effects become significant) and in calibrating all loss factors. Increased accuracy may be obtained by reducing the known noise input level with use of attenuator A. For measurements of noise figure below 3-db, the known noise input level will be provided by means of an accurately calibrated termination, operated at two different temperatures, i.e. the hot-cold loss method.

The noise figure as measured above is not the "spot NF" but represents the average NF between two ranges of frequencies separated by twice the IF frequency. The width of the range of frequencies is a function of the IF bandwidth. This NF, measured without a filter to remove one of the sidebands, is either higher than the minimum "spot NF" or equal to it.



Item	Remarks
A	Waveguide Noise Source Waveguide No. 2200-2 or Equivalent
B	RF Attenuators Standard Telephone and Cables, Ltd. Model 74600 or Equivalent
C	TWT under Test
D	Standard Microwave Test Receiver (I.F. $\approx$ 30 mc)
E	Hewlett-Packard Noise Meter, Model 340A, or Equivalent

Fig. 22 — Block diagram of noise-figure measurement setup.